Developmental Cell

CellPress
OPEN ACCESS

Article

γ-secretase promotes *Drosophila* postsynaptic development through the cleavage of a Wnt receptor

Lucas J. Restrepo,[1,2] Alison T. DePew,[1] Elizabeth R. Moese,[1] Stephen R. Tymanskyj,[1] Michael J. Parisi,[1] Michael A. Aimino,[1] Juan Carlos Duhart,[1] Hong Fei,[1] and Timothy J. Mosca[1,3,*]

[1]Department of Neuroscience, Vickie and Jack Farber Institute of Neuroscience, Thomas Jefferson University, Bluemle Life Sciences Building, Philadelphia, PA 19107, USA

[2]Present address: Department of Molecular, Cell and Cancer Biology, University of Massachusetts Chan Medical School, Worcester, MA 01605, USA

[3]Lead contact

*Correspondence: timothy.mosca@jefferson.edu

https://doi.org/10.1016/j.devcel.2022.05.006

SUMMARY

Developing synapses mature through the recruitment of specific proteins that stabilize presynaptic and postsynaptic structure and function. Wnt ligands signaling via Frizzled (Fz) receptors play many crucial roles in neuronal and synaptic development, but whether and how Wnt and Fz influence synaptic maturation is incompletely understood. Here, we show that Fz2 receptor cleavage via the γ-secretase complex is required for postsynaptic development and maturation. In the absence of γ-secretase, *Drosophila* neuromuscular synapses fail to recruit postsynaptic scaffolding and cytoskeletal proteins, leading to behavioral deficits. Introducing *presenilin* mutations linked to familial early-onset Alzheimer's disease into flies leads to synaptic maturation phenotypes that are identical to those seen in null alleles. This conserved role for γ-secretase in synaptic maturation and postsynaptic development highlights the importance of Fz2 cleavage and suggests that receptor processing by proteins linked to neurodegeneration may be a shared mechanism with aspects of synaptic development.

INTRODUCTION

Developing robust synaptic connections requires a series of events following incipient neuronal contact, culminating in a maturation process to recruit specialized receptor, scaffolding, cytoskeletal, and neurotransmitter-related proteins (Chia et al., 2013). To transit from nascent contact to reliable connection, postsynaptic protein recruitment is especially essential to ensure function. Underscoring the importance of maturation, its failure can lead to neurodevelopmental (Zoghbi and Bear, 2012) and possibly even neurodegenerative (Barnat et al., 2020) disorders. Although postsynaptic maturation requires activity-dependent refinement (Hooks and Chen, 2020; Vonhoff and Keshishian, 2017) and synapse-to-nucleus signals (Marcello et al., 2018), the underlying molecular mechanisms are incompletely understood.

In invertebrates and vertebrates, Wnts generally promote axon guidance, circuit assembly, and neurodevelopment (Fradkin et al., 2005; Salinas and Zou, 2008). At synapses, secreted Wnt ligands signal through multiple Frizzled (Fz), Ryk, and PCP receptor families (Zou, 2020) to engage multiple downstream pathways that regulate synaptic structure, cytoskeletal organization, and activity-dependent function (Budnik and Salinas, 2011). Consistent with a central role in synapse development, loss of synaptic Wnts underlies multiple neurological disorders (Oliva et al., 2018) including Alzheimer's disease (AD) (Tapia-Rojas and Inestrosa, 2018). However, despite the critical importance of synaptic Wnts, the divergent complexity of presynaptic and postsynaptic Wnt signals has precluded understanding of how each downstream pathway influences development and disease.

The *Drosophila* larval neuromuscular junction (NMJ) is a powerful synapse for studying synaptic development and maturation (Harris and Littleton, 2015). The NMJ combines the accessibility of a developing synapse with stereotyped connections (Keshishian et al., 1996) and a myriad of genetic tools aimed at understanding cell-type specific function of genes and processes (Venken et al., 2011a). As a glutamatergic synapse, the *Drosophila* NMJ shares mechanistic conservation with mammalian central synapses (Collins and DiAntonio, 2007), allowing for *Drosophila* discoveries to inform vertebrate biology (Charng et al., 2014) and, in particular, postsynaptic maturation (Chou et al., 2020). At the fly NMJ, synaptic boutons form via activity-dependent motoneuron outgrowth (Ataman et al., 2008; Piccioli and Littleton, 2014; Zito et al., 1999). Nascent, immature boutons contain presynaptic membrane and vesicles but lack postsynaptic apposition—these boutons are termed "ghost boutons" and are transient features of normal synaptic growth and

Please cite this article in press as: Restrepo et al., γ-secretase promotes *Drosophila* postsynaptic development through the cleavage of a Wnt receptor, Developmental Cell (2022), https://doi.org/10.1016/j.devcel.2022.05.006

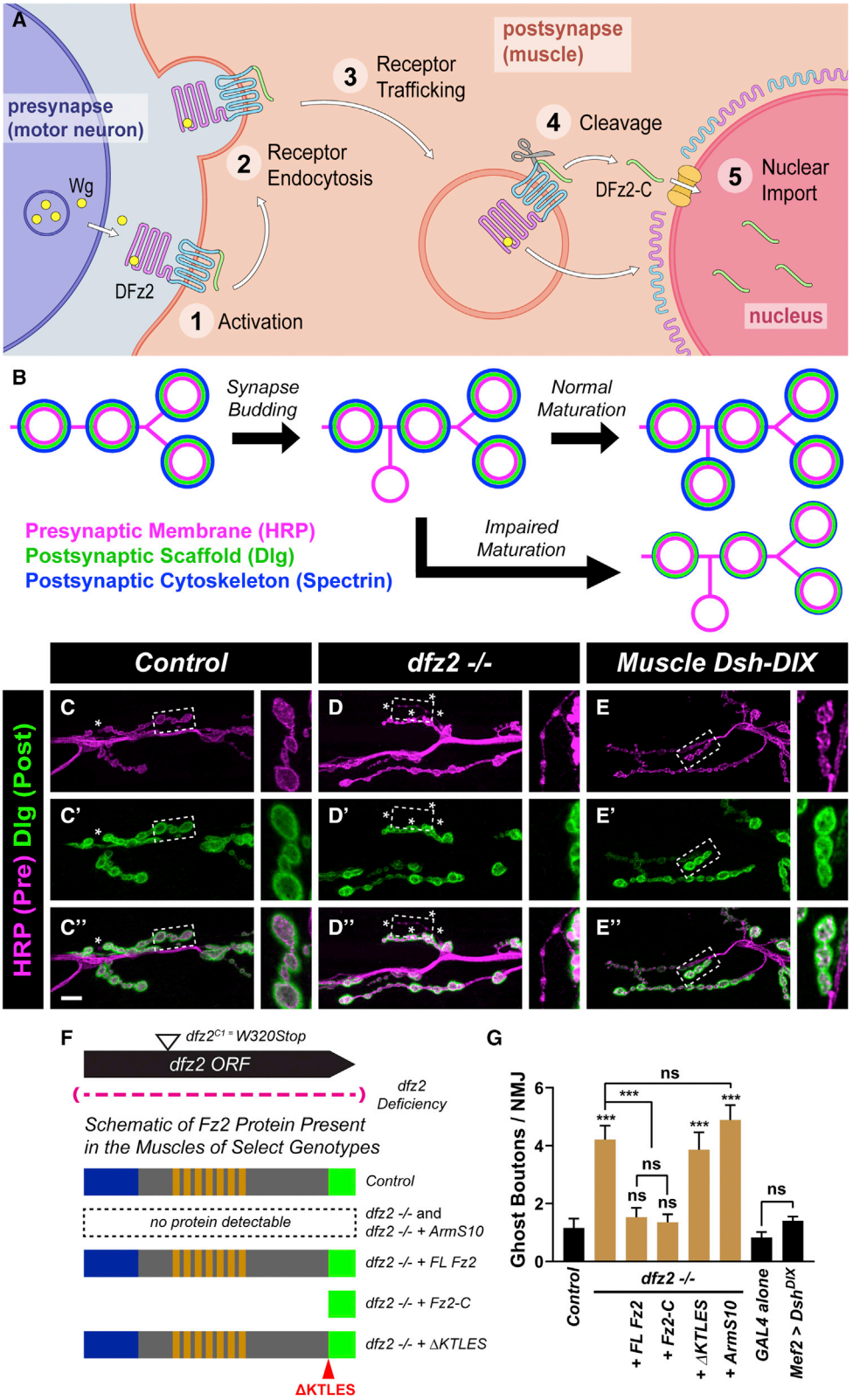

Figure 1. Cleavage of Frizzled2 and the Frizzled nuclear import (FNI) pathway promotes postsynaptic development and maturation

(A) Schematic of *Drosophila* FNI. Presynaptic Wingless activates postsynaptic Fz2, which is then endocytosed, trafficked, and the C-terminus cleaved and imported into the nucleus, whereas the N-terminus remains perinuclear.

(legend continued on next page)

Please cite this article in press as: Restrepo et al., γ-secretase promotes *Drosophila* postsynaptic development through the cleavage of a Wnt receptor, Developmental Cell (2022), https://doi.org/10.1016/j.devcel.2022.05.006

plasticity (Ataman et al., 2008; Piccioli and Littleton, 2014; Vasin et al., 2019). As the larva matures, boutons complete development by recruiting active zones, neurotransmitter release machinery (Fouquet et al., 2009), and postsynaptic receptor, scaffolding, and cytoskeletal proteins (Mosca and Schwarz, 2010a; Schmid et al., 2006, 2008). Examining how ghost boutons may persist and postsynaptic proteins are recruited during late larval stages provides a unique opportunity to separate and characterize the mechanisms of later synaptic maturation from those of earlier synapse formation and growth.

At the fly NMJ, Wnts can promote postsynaptic development via a noncanonical Frizzled nuclear import (FNI) pathway (Figure 1A). Wingless (Wg) is secreted from motoneurons (Ataman et al., 2008) and glia (Kerr et al., 2014) in an activity-dependent mode and binds to postsynaptic muscle Fz2 receptors (Packard et al., 2002). Fz2 is then endocytosed and trafficked to the perinuclear space where the Fz2 C terminus (Fz2-C) is cleaved and imported into the nucleus to regulate expression of genes linked to synaptic development (Ashley et al., 2018; Ataman et al., 2006, 2008; Kamimura et al., 2013; Korkut et al., 2009; Mathew et al., 2005; Mosca and Schwarz, 2010a; Speese et al., 2012). Although the role of Wnts in promoting general synaptic development is evident, the precise aspects controlled by and the physiological relevance of FNI remain controversial. First, it is unclear if FNI promotes general synaptic growth (Mathew et al., 2005) or postsynaptic maturation (Ataman et al., 2006; Kamimura et al., 2013; Mosca and Schwarz, 2010a; Speese et al., 2012). Second, the amino acids that comprise the Fz2 cleavage site overlap with residues that bind Disheveled (Dsh; Axelrod et al., 1998); mutations in those residues thus cannot distinguish between failure of FNI or of a Dsh-dependent, canonical Wnt pathway (Miech et al., 2008). Finally, and perhaps most importantly, the protease that promotes Fz2 cleavage remains unknown; the lack of such knowledge has precluded direct study of cleavage to understand how proteolysis gates postsynaptic maturation. These facets have precluded thorough understanding of the gatekeepers of FNI-dependent neurodevelopment and any evolutionarily conserved synaptic aspects.

To address such gaps, we tested the hypothesis that Fz2 cleavage and FNI promote postsynaptic maturation and subsequently sought to identify the relevant protease. Here, we find that Fz2 cleavage is required for postsynaptic development and maturation at the *Drosophila* NMJ and that γ-secretase, a proteolytic complex linked to AD, is required for Fz2 cleavage and FNI-mediated maturation. Loss of γ-secretase impairs postsynaptic apposition and coordinated behavior and is suppressed by activating the FNI pathway, suggesting that the physiologically relevant cleavage event missing in γ-secretase mutants is that of postsynaptic Fz2. We also find that postsynaptic maturation defects are present in *presenilin* (the catalytic subunit of γ-secretase) mutations associated with AD patients. These data not only highlight a previously unappreciated developmental role for γ-secretase and its downstream mechanism but address longstanding questions of how Fz2 promotes synaptic maturation. Our work also indicates that defects in postsynaptic development are present in AD models, suggesting potentially shared mechanisms among genes linked to development and degeneration.

RESULTS

Fz2 cleavage is required to promote normal synaptic maturation

Synaptic boutons initially form by presynaptic membrane budding (Zito et al., 1999) and subsequently mature via the recruitment of and subsequent apposition by postsynaptic components (Figure 1B) like Discs large/PSD-95 (Budnik et al., 1996), glutamate receptors (Rasse et al., 2005; Schmid et al., 2008), and cytoskeletal proteins (Blunk et al., 2014). Maturation failures result in "ghost boutons" (Figure 1B), which are discrete synaptic endings where the presynaptic bouton persists but lacks postsynaptic components (Ataman et al., 2006). Mutations that perturb postsynaptic NMJ maturation increase ghost boutons and impair cytoskeletal recruitment (Ataman et al., 2008; Harris et al., 2016; Mosca and Schwarz, 2010a; Speese et al., 2012).

Drosophila Fz2 promotes multiple aspects of presynaptic and postsynaptic development (Mathew et al., 2005; Mosca and Schwarz, 2010a), but how it promotes synaptic maturation is unclear. Loss of *fz2* increases ghost boutons (Mosca and Schwarz, 2010a), indicating the receptor is required for normal maturation (Figures 1C, 1D, and 1G). Moreover, Fz2-C nuclear entry is required for normal postsynaptic development and gene expression (Mosca and Schwarz, 2010a; Speese et al., 2012). It is unclear if blocking Fz2 cleavage specifically impairs maturation. To test if cleavage is required for normal postsynaptic development, we used a molecular replacement approach (Figure 1F) by expressing Fz2 transgenes (Mathew et al., 2005) that encode the full-length receptor (FL-Fz2), a noncleavable receptor (ΔKTLES), or the receptor C terminus (Fz2-C) only in the postsynaptic muscles of *fz2* mutants. FL-Fz2 or Fz2-C rescued the developmental defect but ΔKTLES did not (Figures 1F and 1G), indicating that the residues comprising the cleavage site are required for Fz2-mediated synaptic maturation. However, the KTLES sequence also binds Dsh, a canonical Wnt signaling protein (Axelrod et al., 1998) found at the developing postsynapse (Miech et al., 2008). Thus, removing KTLES cannot, by itself, distinguish between noncanonical Fz2 cleavage and canonical Dsh-dependent function in development. To explicitly test

(B) Schematic of NMJ bouton addition. Presynaptic boutons (magenta) are surrounded by postsynaptic discs large (green) and the cytoskeleton (blue). When maturation is impaired, there are more ghost boutons and reduced spectrin thickness at all boutons.
(C–E) Representative images of NMJs from *Control* (C), *dfz2* mutant (D), and muscle-expressing Dsh-DIX larvae (E) stained with antibodies to HRP (magenta) and Dlg (green). Asterisks indicate ghost boutons; insets represent high magnification (dashes).
(F) Diagram of the *dfz2* genomic region with the null $dfz2^{C1}$ allele and *dfz2* deficiency. Schematic of Fz2 constructs used for experiments, highlighting the genotypes and the Fz2 protein in muscles of select genotypes, be it endogenous (control) or transgenic.
(G) Quantification of ghost boutons.
For all experiments, data = mean ± SEM with significance calculated by ANOVA followed by Tukey's test for multiple comparisons. n ≥ 6 larvae, 12 NMJs. ***p < 0.001, n.s. = not significant. Scale bars, 10 μm, 5 μm (insets).

Please cite this article in press as: Restrepo et al., γ-secretase promotes *Drosophila* postsynaptic development through the cleavage of a Wnt receptor, Developmental Cell (2022), https://doi.org/10.1016/j.devcel.2022.05.006

canonical Fz2 signaling in maturation, we first examined if blocking downstream Wnt signals through Dsh would perturb postsynaptic development by expressing dominant-negative Dsh in muscles. Disrupting muscle Dsh did not affect ghost bouton number (Figures 1E and 1G), suggesting Dsh is dispensable for maturation. We next expressed Arm^{S10}, an activated Armadillo, in *fz2* null mutant muscles to determine if activating canonical Wg signaling downstream of Dsh-suppressed *fz2* synaptic maturation defects. Arm^{S10} failed to suppress the increase in ghost boutons in *fz2* null mutants (Figure 1G), further suggesting that canonical Wg signaling is dispensable for maturation. Thus, the failed postsynaptic development seen when the KTLES site is mutated (Figure 1G) is likely due to failed Fz2-C cleavage, highlighting a role in postsynaptic maturation.

An *in vivo* screen to identify proteases involved in synaptic maturation

The Fz2 KTLES cleavage site is a glutamyl endopeptidase site (Mathew et al., 2005) and is required for postsynaptic development (Figure 1G). To identify proteases responsible for Fz2 cleavage, we performed a tissue-specific RNAi screen (Dietzl et al., 2007) against candidates predicted by GO-term analysis to have glutamyl endopeptidase activity (Figure 2A). We reasoned muscle-specific RNAi would (1) target the appropriate tissue as Fz2 is expressed in muscle and (2) positive hits would phenocopy *fz2* mutants. As such, we stained larval NMJs for presynaptic and postsynaptic markers (HRP and Dlg) and quantified ghost boutons. We also quantified "footprint" boutons, which occur when the presynaptic NMJ degenerates, leaving behind postsynaptic Dlg (Eaton and Davis, 2005) and can denote synaptic destabilization, distinguishing developmental defects from degeneration. On average, control larvae (expressing RNAi against GFP) had 0.82 ± 0.12 ghost bouton at the muscle 6/7 NMJ (Figures 2B and 2C); a positive screen hit was denoted by a statistically significant increase in ghost bouton number. We quantified ghost and footprint boutons in 93 candidates (Table S1) and controls (Figure 2B). In positive controls expressing RNAi against *dfz2* or *trol*, which is required for NMJ Wnt signaling (Kamimura et al., 2013), we observed 3-fold more ghost boutons (Figure 2E), indicating impaired postsynaptic maturation. Only two other RNAi lines (Figures 2D and 2E) increased ghost bouton number, those targeting *presenilin* and *nicastrin*. Neither *presenilin* nor *nicastrin* RNAi influenced "footprint" boutons (Figure 2B), suggesting impaired maturation but not destabilization. Presenilin (Psn) and Nicastrin (Nct), along with Aph-1 and Pen-2, comprise γ-secretase, a proteolytic holocomplex whose function is linked to Alzheimer's Disease (AD), a devastating neurodegenerative disorder (De Strooper et al., 2012). Mutations in *PSEN1*, the human *psn* homolog, are the most prevalent genetic cause of early-onset familial AD (Lanoiselée et al., 2017). Our findings raised the possibility that γ-secretase could promote postsynaptic development and maturation via Fz2 cleavage.

Muscle γ-secretase promotes postsynaptic maturation and normal behavior

We next examined whether endogenous γ-secretase localizes to the NMJ. γ-secretase comprises four independent subunits (Figure 3A); Psn (Figure 3B) and Nct (Figure 3D) staining overlapped with HRP staining and Dlg staining, suggesting γ-secretase localizes presynaptically and postsynaptically at the NMJ. Presynaptic Psn is consistent with previous work (Knight et al., 2007) and postsynaptic Psn with our screen results (Figure 2). Specific Psn and Nct immunostaining at the synapse is absent in respective null mutants (Figures 3C and 3E), demonstrating antibody specificity. We also found that muscle-driven, epitope-tagged Psn and Nct can localize to the NMJ (Figures S1A–S1D) and olfactory neuron-driven, epitope-tagged Psn and Nct can localize to central synapses (Figures S1E and S1F). These data indicate that γ-secretase subunits are synaptically localized and comprise a postsynaptic pool at the NMJ.

To determine if loss of Psn and Nct impaired postsynaptic development and maturation, we examined null *psn* and *nct* mutants and quantified ghost bouton number (Figure 4A) and α-spectrin staining intensity (Figure 4F). Each mutant displayed a significant increase in ghost bouton number (Figures 4B–4E) and markedly reduced α-spectrin (Figures 4G–4J), indicating impaired postsynaptic maturation. This independently recapitulated our screen results (Figure 2). We observed similar ghost bouton and α-spectrin defects in both *aph-1* and *pen-2* mutants, demonstrating that loss of any γ-secretase subunit phenocopies each other (Figure S2). In all mutants (*psn*, *nct*, *aph-1*, and *pen-2*), bouton number, muscle area, active zone and glutamate receptor density, and synaptic protein levels remained unchanged (Figure S3), suggesting maturation defects were not secondary to general failures of development including synapse formation, innervation, or axon guidance. To assess if the observed defects in postsynaptic development were due to the loss of the enzymatic function of γ-secretase, we examined if blocking γ-secretase activity perturbed bouton maturation. When wild-type flies were fed the γ-secretase inhibitor L685,458 (Liu et al., 2018), they showed 5-fold more ghost boutons (Figures S4A–S4D). L685,458 did not enhance the *psn* ghost bouton phenotype (Figures S4C and S4D), suggesting absent γ-secretase activity underlies failed maturation.

Given that Psn and Nct are expressed presynaptically and postsynaptically, we next sought to determine which pool promoted effective postsynaptic maturation. Using tissue-specific rescue of each mutant with epitope-tagged transgenes (Stempfle et al., 2010), we found that presynaptic expression of γ-secretase in motoneurons of the respective mutant could not rescue the postsynaptic development and maturation defects (Figures 4E and 4J) nor could neuronal RNAi induce defects (Figure 4J). Expression in postsynaptic muscles, however, completely suppressed the respective mutant defects (Figures 4E and 4J). We also observed the same rescue of maturation phenotypes with muscle expression of the respective transgene in *aph-1* and *pen-2* mutants (Figures S2E and S2J), indicating that all four γ-secretase subunits are required postsynaptically for proper synaptic development and maturation.

Genetic perturbations that impair synaptic maturation often functionally impair synaptic plasticity and coordinated behavior while maintaining largely normal basal physiology (Clement et al., 2012; Hoy et al., 2013; Scharkowski et al., 2018; Wegener et al., 2018). Consistently, *psn* null mutants have normal basal NMJ physiology but impaired plasticity (Knight et al., 2007). To test if known defects in plasticity were accompanied by altered behavior and if such alterations were present in γ-secretase

Please cite this article in press as: Restrepo et al., γ-secretase promotes *Drosophila* postsynaptic development through the cleavage of a Wnt receptor, Developmental Cell (2022), https://doi.org/10.1016/j.devcel.2022.05.006

CellPress
OPEN ACCESS

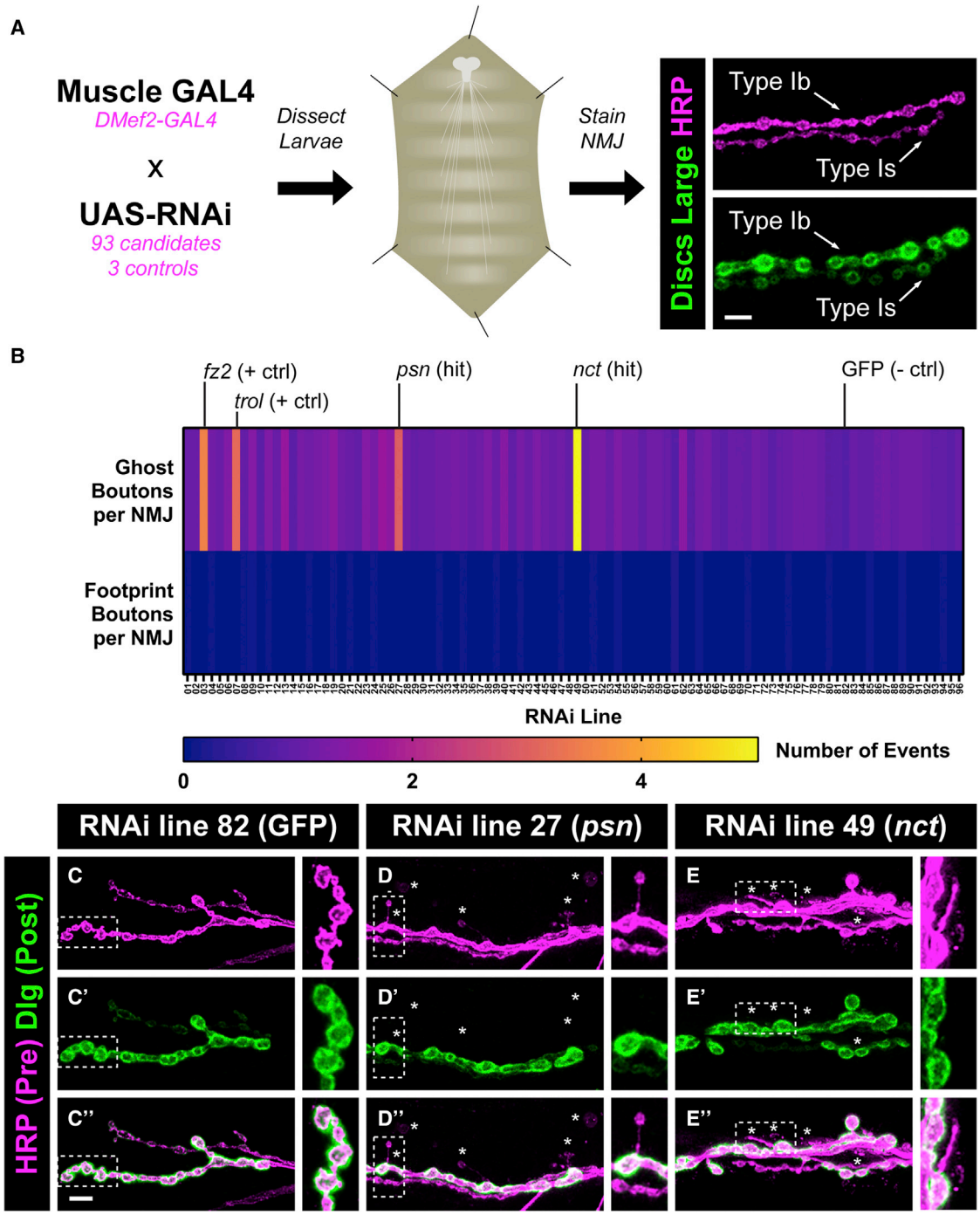

Figure 2. A tissue-specific RNAi screen identifies *presenilin* and *nicastrin* as required for normal postsynaptic development and maturation

(A) RNAi screen: UAS-RNAi candidates or controls were driven using *DMef2-GAL4*. Larvae were dissected and stained with Dlg and HRP antibodies. The representative image shows Dlg and HRP at type Ib and Is boutons.

(B) Heat map of the number of ghost (top) or footprint (bottom) boutons in each RNAi line.

(C–E) Representative images of NMJ boutons stained with antibodies to HRP (magenta) and Dlg (green) in larvae expressing RNAi against GFP (C), *psn* (D), or *nct* (E) in muscles. Asterisks indicate ghost boutons; insets represent high magnification (dashes).

For all experiments, the data represent mean number of events. Significance (Table S1) was calculated by ANOVA followed by Tukey's test for multiple comparisons. For each RNAi, n ≥ 5 larvae, 10 NMJs. Scale bars, 10 μm, 5 μm (insets).

Please cite this article in press as: Restrepo et al., γ-secretase promotes *Drosophila* postsynaptic development through the cleavage of a Wnt receptor, Developmental Cell (2022), https://doi.org/10.1016/j.devcel.2022.05.006

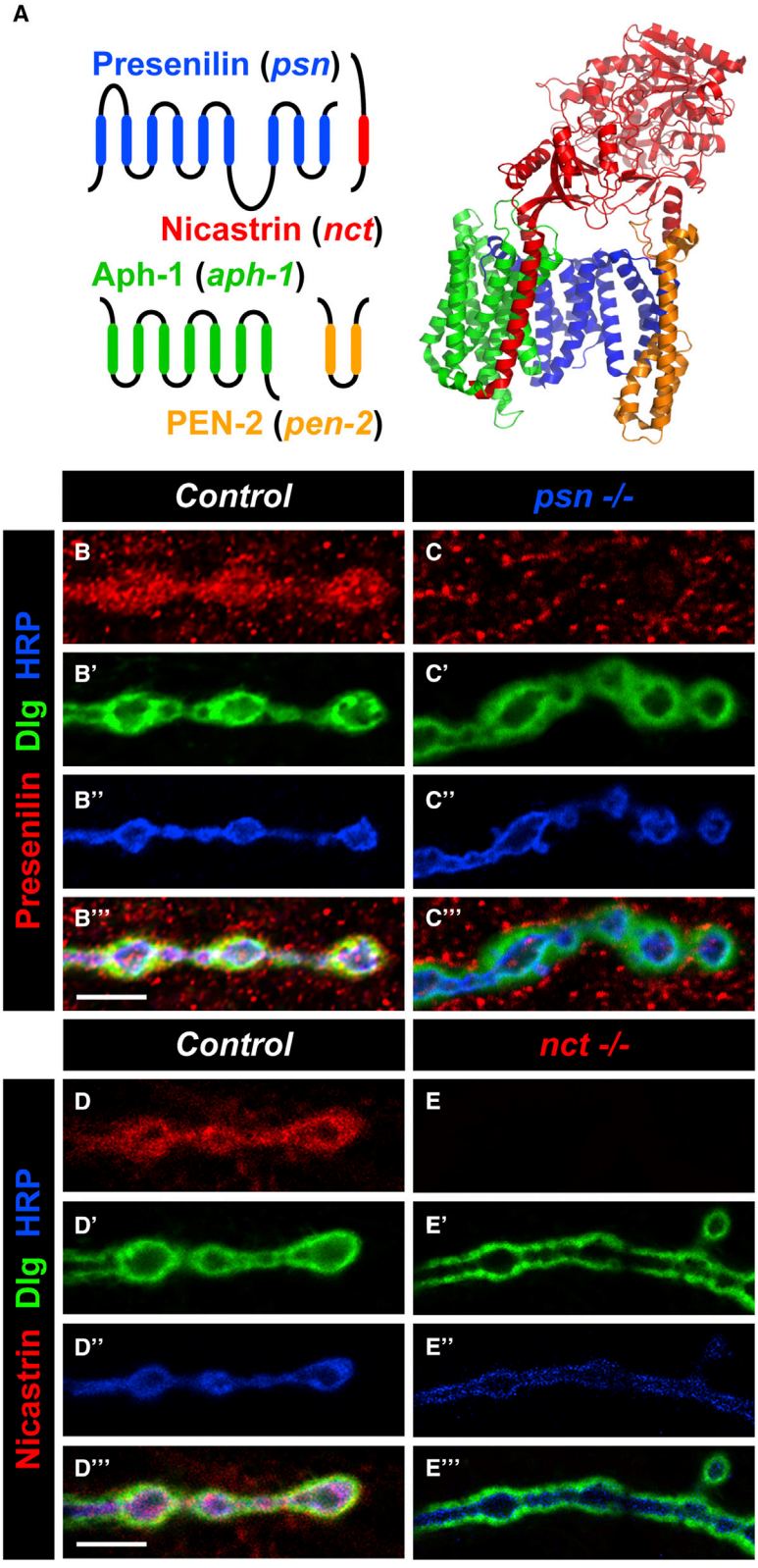

Figure 3. Presenilin and Nicastrin are expressed presynaptically and postsynaptically at developing NMJs

(A) Schematic of γ-secretase subunits (left) and structure (right; Bai et al., 2015). Color coding in all figures denotes mutants of each subunit: Presenilin (blue), Nicastrin (red), Aph-1 (green), and Pen-2 (orange).

(B and C) Representative single confocal section of control (B) or *psn* mutant (C) larvae stained with antibodies to Presenilin (red), Dlg (green), and HRP (blue).

(D and E) Representative single confocal section of control (D) or *nct* mutant (E) larvae stained with antibodies to Nicastrin (red), Dlg (green), and HRP (blue).

Scale bars, 5 μm.

mutants, we assayed larval crawling behavior via mutant analysis and tissue-specific RNAi. Changes in coordinated larval crawling behavior would be consistent with defects in postsynaptic development and maturation. We used locomotion assays (Figures 4J–4O and S2J–S2O) to quantify distance traveled and peristaltic waves as measures of motility along with the number of head sweeps as a measure of scanning behavior (Kane et al., 2013). In all cases, loss of any γ-secretase component reduced distance traveled (Figures 4K and S2K) and peristalsis (Figures 4M and S2M), indicating impaired locomotion. Intriguingly, loss of any γ-secretase component increased head sweeps (Figures 4O and S2O), suggesting an inability to engage the normal behavioral pattern. All three motility phenotypes were fully recapitulated by muscle γ-secretase RNAi, whereas neuronal RNAi showed no phenotype or only mildly impaired distance traveled (Figure 4L), likely due to presynaptic Psn (Knight et al., 2007). The data indicate loss of postsynaptic γ-secretase impairs larval behavior and, with altered morphology, are consistent with failed maturation.

γ-secretase functions in the Fz2 nuclear import pathway to promote cleavage

Our findings indicate roles for Fz2 cleavage and muscle γ-secretase in postsynaptic development, maturation, and function. We next sought to learn if Fz2 cleavage and muscle γ-secretase were also mechanistically connected, with the working model that γ-secretase activity enables Fz2 cleavage. However, given the role of γ-secretase in Notch signaling (Lathia et al., 2008), we first examined if perturbing Notch impaired postsynaptic maturation. If γ-secretase functioned via Notch, we would expect loss of Notch to phenocopy γ-secretase. However, mutations in various Notch genes did not increase ghost boutons (Figures S4E–S4I). Thus, γ-secretase does not promote maturation via Notch.

To begin to connect γ-secretase and Fz2, we used transheterozygous and double mutant analyses to determine if *fz2* and γ-secretase interacted genetically. Single *psn*, *fz2*, or *nct* heterozygotes showed normal postsynaptic maturation (Figures 5A, 5B, and 5D). However, transheterozygous combinations of *psn*, *nct*, and *fz2* significantly increased ghost boutons (Figures 5C and

Please cite this article in press as: Restrepo et al., γ-secretase promotes *Drosophila* postsynaptic development through the cleavage of a Wnt receptor, Developmental Cell (2022), https://doi.org/10.1016/j.devcel.2022.05.006

CellPress
OPEN ACCESS

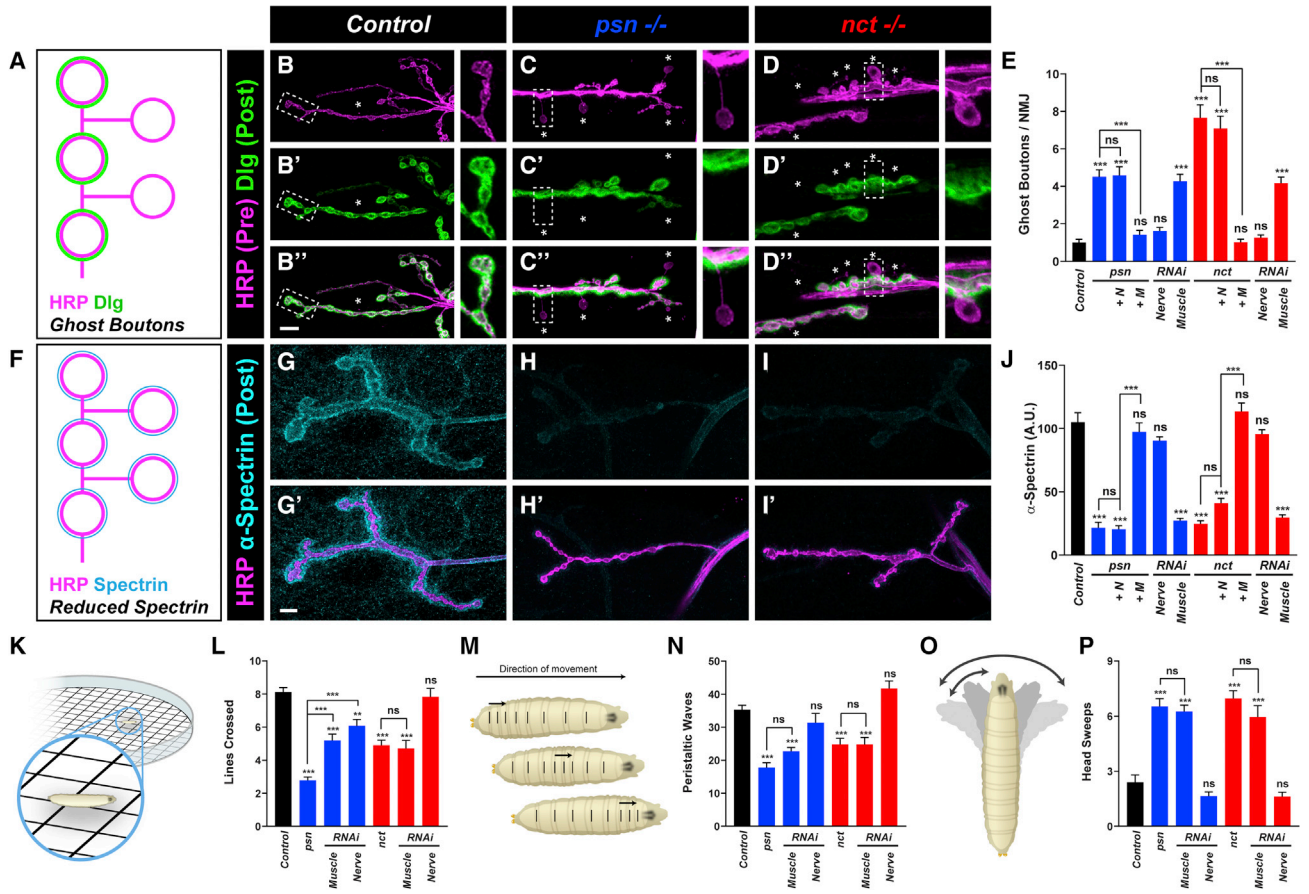

Figure 4. Loss of postsynaptic *psn* or *nct* impairs postsynaptic development and function

(A) Schematic of ghost bouton phenotype in maturation mutants. Normal boutons contain presynaptic HRP (magenta) and postsynaptic Dlg (green) while ghost boutons lack Dlg.

(B–D) Representative images of control (B), *psn* mutant (C), and *nct* mutant (D) larvae stained with antibodies to HRP (magenta) and Dlg (green). Asterisks indicate ghost boutons; insets represent high magnification (dashes).

(E) Quantification of ghost boutons. +N = nerve expression, +M = muscle expression.

(F) Schematic of the reduced spectrin phenotype in maturation mutants: all boutons show reduced spectrin thickness and intensity.

(G–I) Representative images of control (G), *psn* mutant (H), and *nct* mutant (I) larvae stained with antibodies to HRP (magenta) and α-spectrin (cyan).

(J) Quantification of α-spectrin fluorescence. +N = nerve expression, +M = muscle expression.

(K) Diagram of larval crawling assay to measure motility.

(L) Quantification of larval motility in mutant and RNAi genotypes.

(M) Diagram of larval peristaltic waves with arrows indicating direction of movement and lines on the larva denoting body wall segments.

(N) Quantification of peristaltic waves in mutant and RNAi genotypes.

(O) Diagram of the larval head sweep. Arrows and shading indicate directions of motion during the head sweep behavior.

(P) Quantification of head sweeps in mutant and RNAi genotypes.

For all experiments, data = mean ± SEM with significance calculated by ANOVA followed by Tukey's test for multiple comparisons. For (A)–(J), n ≥ 8 larvae, 16 NMJs; for (K)–(P), n ≥ 24 larvae. $^{**}p < 0.01$, $^{***}p < 0.001$, n.s. = not significant. Scale bars, 10 μm, 5 μm (insets).

5D); this genetic interaction was specific, as transheterozygotes between *nct* and *ten-a* (a gene that impairs postsynaptic development independent of Fz2; Mosca et al., 2012) did not influence ghost boutons (Figure 5D). Finally, *aph-1 fz2* double mutants phenocopied single *aph-1* and *fz2* mutants (compare Figures 5D and S2E), further suggesting function in the same, and not a parallel, genetic pathway.

Having observed genetic interactions between γ-secretase and Fz2, we next tested if they could function together physically in a complex, consistent with a role promoting cleavage. We examined the synaptic localization of Fz2, Psn, and Nct with proximity ligation assays (PLAs) to determine if the proteins co-localized within 40 nm (Söderberg et al., 2006). Epitope-tagged Fz2 and Psn localize postsynaptically when expressed only in muscles (Figure 5E) and show a positive PLA signal, suggesting close proximity (Figures 5F and S5A). Importantly, we observed no specific signal in controls (Figures S5B–S5D). We quantified PLA puncta in all experiments (Figures S5A–S5D) and found a 10-fold increase over background in Fz2 / Psn coexpression (Figure S5G), suggesting specific interaction. As the antibodies to endogenous Psn, Nct, and Fz2 were raised in the same animal, we could not assess endogenous colocalization and PLA.

Please cite this article in press as: Restrepo et al., γ-secretase promotes *Drosophila* postsynaptic development through the cleavage of a Wnt receptor, Developmental Cell (2022), https://doi.org/10.1016/j.devcel.2022.05.006

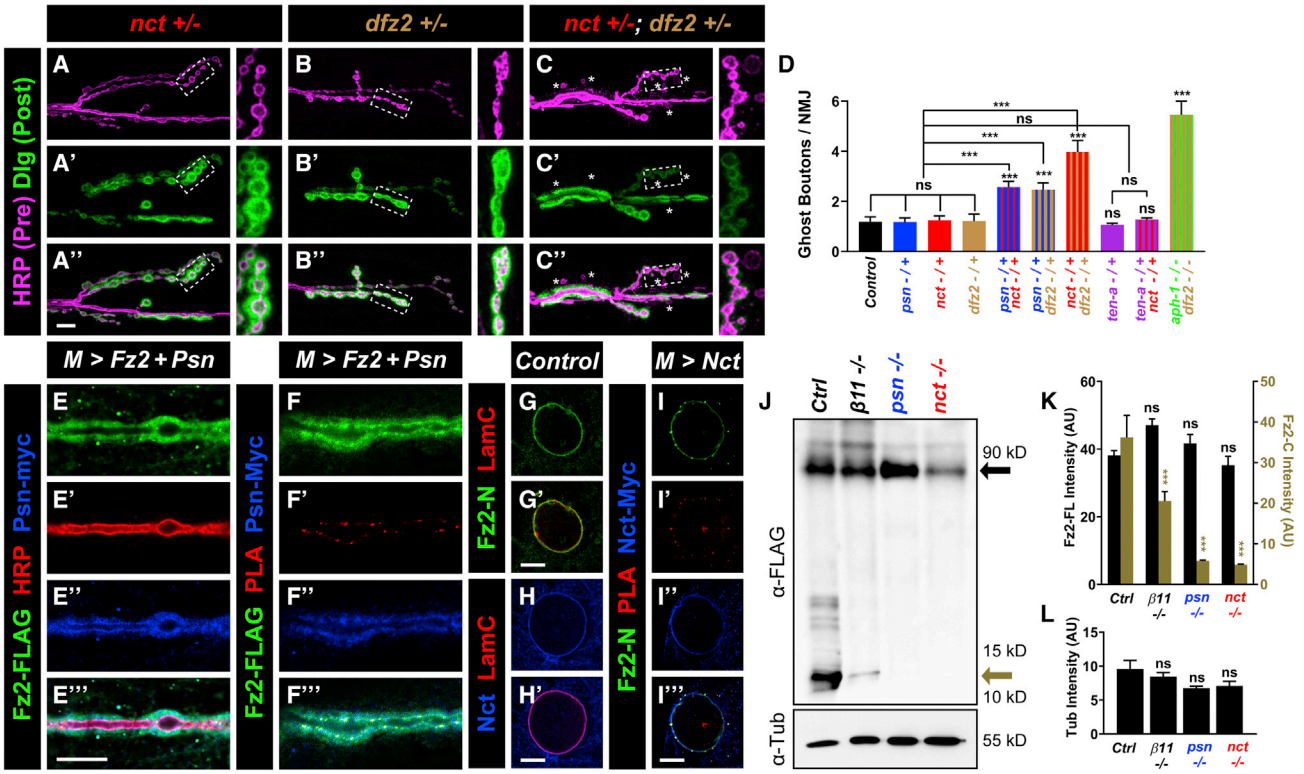

Figure 5. Psn and Nct interact with the Fz2 nuclear import pathway and enable Fz2-C cleavage

(A–C) Representative images of *nct* (A), *dfz2* (B), and *nct; dfz2* heterozygotes (C) stained with antibodies to HRP (magenta) and Dlg (green). Asterisks indicate ghost boutons; insets represent high magnification (dashes).

(D) Quantification of ghost boutons in mutant and transheterozygous phenotypes.

(E) Representative images of larvae expressing Fz2-FLAG and Psn-Myc in postsynaptic muscles, stained for antibodies to FLAG (green), Myc (blue), and HRP (red).

(F) Representative images of larvae expressing Fz2-FLAG and Psn-Myc in postsynaptic muscles, stained for antibodies to FLAG (green) and Myc (blue) and reacted with a proximity ligation assay (red).

(G and H) Single section images of larval muscle nuclei and stained with antibodies to Fz2-N (G, green) or Nct (H, blue), and Lamin C (red) to mark the nuclear envelope.

(I) Representative images of larvae expressing Nct-Myc in muscle, stained with antibodies to Fz2-N (green), Myc (blue), and reacted with a proximity ligation assay (red).

(J) Western blot analysis of muscle-expressed Fz2-FLAG cleavage in *control*, *imp-β11* mutant, *psn* mutant, and *nct* mutant larvae. Full-length Fz2 (**) and Fz2-C (*) are denoted. Tubulin is used as a loading control.

(K) Graph of α-FLAG band intensity (Fz2-FL, Black; Fz2-C, gold) from experiments in (J).

(L) Quantification of α-tubulin band intensity from experiments in (J).

For all experiments, data = mean ± SEM with significance calculated by ANOVA followed by Tukey's test for multiple comparisons. For (A)–(D), n ≥ 6 larvae, 12 NMJs per genotype; for (E)–(L), representative images and quantifications are from n ≥ 3 experiments. ***p < 0.001. n.s. = not significant. Scale bars, 10 μm, 5 μm (insets).

However, we performed analogous PLA experiments using endogenous Psn with muscle-expressed Fz2-FLAG (Figure S5E) and endogenous Fz2 with muscle-expressed Psn-Myc (Figure S5F). In all cases, we observed positive postsynaptic signal significantly over background (Figures S5E–S5I), suggesting the endogenous version of each protein localizes near its exogenously expressed partner.

Endogenous Fz2 (Mathew et al., 2005) and Nct also localize to the nuclear periphery (Figures 5G and 5H), where Fz2 cleavage likely occurs (Kim et al., 2021; Mathew et al., 2005). We detected positive PLA signal between Fz2 and Nct at the nuclear envelope (Figure 5I), indicating proximity at the predicted Fz2 cleavage location. We also saw similar nuclear colocalization using postsynaptically expressed Fz2 and Psn (Figure S5J).

Fz2 trafficking to the nucleus requires endocytosis (Mathew et al., 2005) and endosomal trafficking (Kim et al., 2021) before being cleaved and imported into the nucleus via Imp-β11 (Mosca and Schwarz, 2010a). As we observed synaptic colocalization of Psn and Fz2 (Figures 5E and S5G) at the nucleus (Figures 5G and 5H), we next asked if the two trafficked together. Consistent with coincident trafficking, we observed Psn and Fz2 colocalization with the early endosome marker Rab5 (Figure S5K) near the synapse (but not the nucleus) and with the late endosome marker Rab7 (Figure S5L) near the nucleus (but not the synapse). Intriguingly, we observed nonsynaptic PLA signal (Figures S5E and S5F) with Fz2 and Psn that may represent trafficking puncta. Finally, Psn and Fz2 colocalized with Imp-β11 at postsynaptic nuclei (Figure S5M). These results suggest that Psn (and thus,

Please cite this article in press as: Restrepo et al., γ-secretase promotes *Drosophila* postsynaptic development through the cleavage of a Wnt receptor, Developmental Cell (2022), https://doi.org/10.1016/j.devcel.2022.05.006

γ-secretase) colocalizes with and traffics similarly to Fz2, consistent with their interactions.

Both the genetic and proximity interactions between Fz2 and γ-secretase suggested their coordinated involvement. If γ-secretase is required for Fz2 cleavage, we hypothesized that loss of γ-secretase would (1) impair Fz2-C cleavage in a detectable manner and (2) result in abrogated nuclear Fz2-C entry (Figure 1A), as Fz2-C cleavage is required for nuclear import (Mathew et al., 2005). We first sought to determine where the FNI pathway was perturbed using antibodies to Wg and to the N-termini (Fz2-N) and C-termini (Fz2-C) of Fz2 (Mathew et al., 2005). Wg expression (Figures S6A–S6D) and Fz2 expression, trafficking, and endocytosis (Figures S6E–S6H) are all unchanged by the loss of γ-secretase, indicating no impairments upstream of the nucleus. We next assayed nuclear Fz2-C staining, which is indicative of successful cleavage and import. Although nuclear Fz2-C puncta are evident in control samples (Figure S6I), loss of *psn* or *nct* abrogated nuclear Fz2-C staining (Figures S6J and S6K). The loss of nuclear Fz2-C puncta was suppressed by muscle, but not neuronal, expression of Psn or Nct in the respective mutant background (Figure S6L), consistent with postsynaptic γ-secretase functioning in Fz2-C cleavage. To directly assess Fz2 cleavage, we expressed a C-terminally FLAG-tagged Fz2 in muscles of control, *psn*, or *nct* mutant larvae and examined the receptor via western blot of larval body-wall lysates. In control samples (Figure 5J), we observed both FLAG-tagged full-length (90 kDa) and Fz2-C bands (12 kDa). The full-length bands were also present in *psn* and *nct* mutants but cleaved Fz2-C was absent, indicating failed cleavage (Figure 5J). Moreover, *imp-β11* mutants, which block Fz2-C nuclear entry (Figure 5J), show Fz2-C cleavage (Figure 5J), suggesting absent cleavage is not a byproduct of failed import. We quantified Fz2-FL and Fz2-C band intensity and found that Fz2-FL is unchanged across genotypes (Figures 5K and 5L), whereas Fz2-C intensity is reduced by 88% in both *psn* and *nct* mutants (Figure 5K). Fz2-C intensity is decreased by 47% in the *imp-β11* mutant (Figure 5K); this may be due to Fz2-C destabilization in the absence of nuclear import. Taken together, our data indicate that γ-secretase is required for the cleavage and subsequent nuclear import of Fz2.

Typically, direct γ-secretase cleavage occurs in the plane of the membrane after ectodomain shedding (Güner and Lichtenthaler, 2020). As Fz2 is unlikely to undergo ectodomain shedding (Kim et al., 2021; Mathew et al., 2005; Mosca and Schwarz, 2010a) and γ-secretase cleaves diverse targets (Güner and Lichtenthaler, 2020), we surmised that cleavage site proximity to the membrane may influence cleavage, consistent with Fz2 as a direct target of γ-secretase. Using structural modeling, we constructed a model of *Drosophila* Fz2 (Figure S6M). The KTLES cleavage site immediately follows the seventh transmembrane (TM7) domain and presents hydrophobic side chains to the membrane. This raises the possibility that although the cleavage site is cytoplasmic, it may interact with and remain juxtaposed to the membrane. This could allow the site to be recognized by γ-secretase (Güner and Lichtenthaler, 2020; Xie et al., 2014). As Fz2 cleavage is required for postsynaptic maturation, we reasoned that increasing the distance between TM7 and KTLES (although retaining the cleavage site) would impair Fz2 function, presumably by perturbing cleavage. To test this, we built a transgenic Fz2 receptor with 5 alanine residues (Fz2 + 5A) inserted between TM7 and KTLES and expressed it in muscles of *fz2* mutants. Although postsynaptic full-length Fz2 rescues the ghost bouton increase in *fz2* mutants (Figure 1), Fz2 + 5A failed to suppress the phenotype (Figures S6N–S6P). This indicates that altering the membrane to cleavage site distance blocks Fz2 from promoting maturation, consistent with Fz2 as a direct cleavage target of γ-secretase.

Restoring nuclear Fz2-C suppresses maturation defects in γ-*secretase* mutants

Our data indicate roles for muscle γ-secretase in postsynaptic maturation and Fz2 cleavage (Figure 6A). However, γ-secretase has multiple cleavage targets (Wolfe, 2009), all of which would be absent in a γ-*secretase* mutant. Therefore, we tested whether the causative event underlying failed maturation in γ-*secretase* mutants (Figure 6A′) was the absence of cleaved, nuclear Fz2-C (Mathew et al., 2005; Mosca and Schwarz, 2010a; Speese et al., 2012). If so, we reasoned that restoring nuclear Fz2-C to γ-*secretase mutant* muscle nuclei (Figure 6A″) would restore normal maturation. To do so, we expressed tagged Fz2-C (Kamimura et al., 2013; Mathew et al., 2005; Mosca and Schwarz, 2010a) with a nuclear localization signal (myc-NLS-Fz2-C) in *psn* or *nct* mutant muscles and assayed the morphological and behavioral phenotypes that accompany impaired maturation. In all cases, muscle Fz2-C expression suppressed the ghost bouton (Figures 6B–6F and 6L), α-spectrin (Figures 6G–6K and 6M), and behavioral alterations (Figures 6N–6P) in *psn* and *nct* mutants. A similarly targeted GFP transgene did not suppress the defects (Figures 6C, 6E, 6H, 6J, 6L–6P), demonstrating the specificity of Fz2-C. These data indicate that the major relevant event underlying the postsynaptic maturation phenotypes associated with γ-secretase loss is the absence of cleaved, nuclear Fz2-C.

γ-secretase perturbation affects *Drosophila* central synapse development

We next asked if the role of γ-secretase in synaptic development and maturation was conserved at central synapses and evolutionarily across species. To examine this in the *Drosophila* brain, we expressed γ-secretase RNAi in olfactory receptor neurons (ORNs) and quantified active zone number in the antennal lobe (Mosca and Luo, 2014). In the antennal lobe, mature synaptic organization is not marked by ghost boutons but by the establishment of a stable active zone number by 10 days posteclosion (Mosca and Luo, 2014; Mosca et al., 2017). We quantified ORN active zones using Brp-Short and neurite volume via mCD8-GFP (Mosca and Luo, 2014) and observed 17%–23% fewer Brp-Short puncta with *psn*, *nct*, or *aph-1* RNAi (Figures S7A–S7D, S7I, and S7K). Neurite volume was unaffected (Figures S7E–S7H, S7J, and S7L), suggesting that ORN wiring was unimpaired, and the active zone defect specific. These data suggest that at fly central synapses, γ-secretase also establishes mature synaptic organization, consistent with conservation from NMJs.

γ-secretase activity promotes dendritic spine maturation in mammalian neurons

Mammalian γ-secretase promotes dendritic spine development, neuroprotection, and cell contact (Barthet et al., 2013; Fazzari

Please cite this article in press as: Restrepo et al., γ-secretase promotes *Drosophila* postsynaptic development through the cleavage of a Wnt receptor, Developmental Cell (2022), https://doi.org/10.1016/j.devcel.2022.05.006

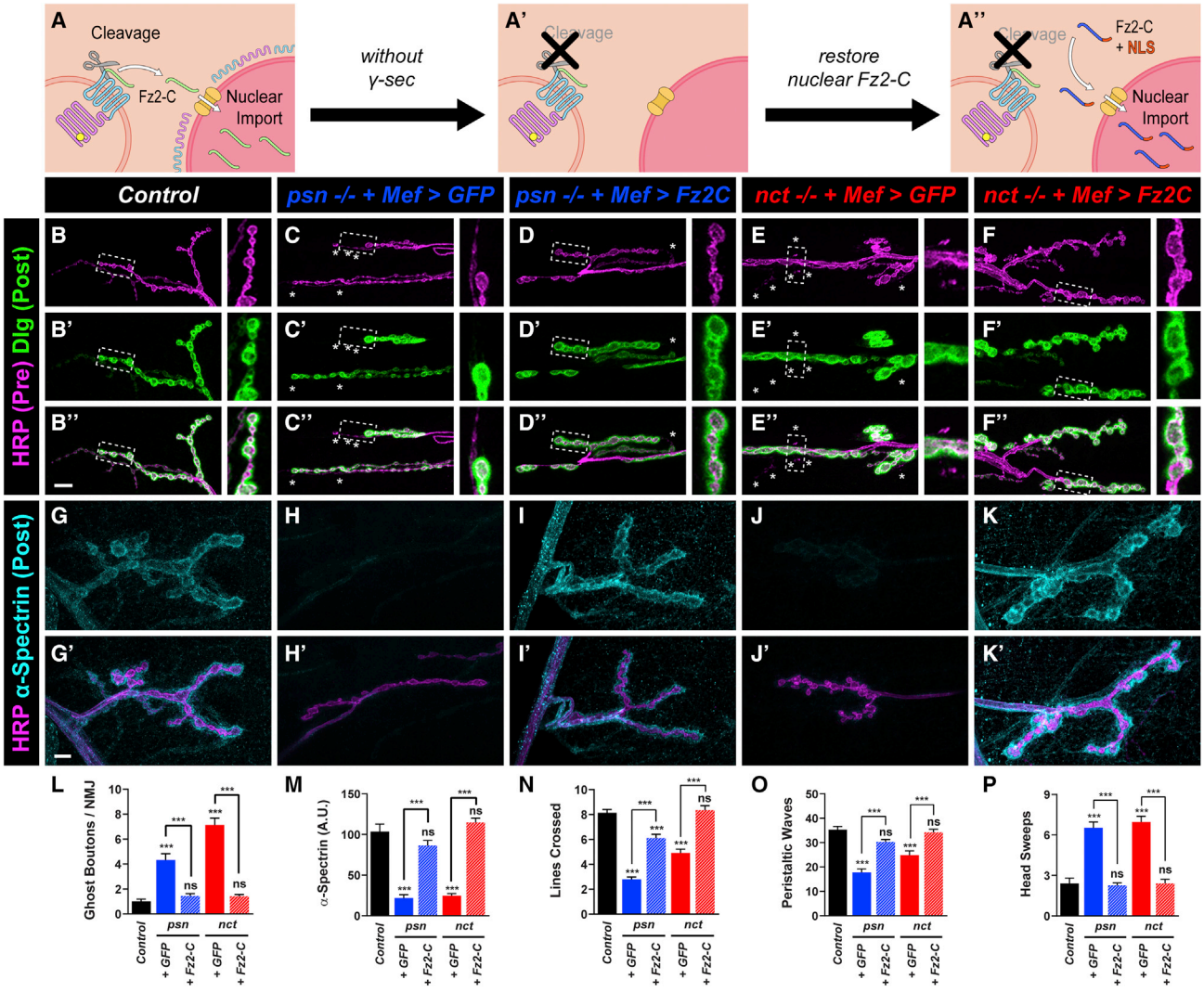

Figure 6. Restoration of nuclear Fz2-C suppresses the developmental phenotypes of *psn* and *nct* mutants

(A) Hypothesis: normal development accompanies Fz2-C cleavage and nuclear entry (A); development is impaired when Fz2-C nuclear entry is prevented due to loss of γ-secretase activity (A′); if precleaved Fz2-C is expressed in muscles, it should bypass the need for γ-secretase and restore normal development (A″).

(B–F) Representative images of control larvae (B), *psn* mutant larvae expressing NLS-GFP (C) or NLS-Fz2-C (D) in muscles, and *nct* mutant larvae expressing NLS-GFP (E) or NLS-Fz2-C (F) in muscles and stained with antibodies to HRP (magenta) and Dlg (green). Asterisks indicate ghost boutons; insets represent high magnification (dashes).

(G–K) Representative images of control larvae (G), *psn* mutant larvae with NLS-GFP (H) or NLS-Fz2-C (I) in muscles, and *nct* mutant larvae with NLS-GFP (J) or NLS-Fz2-C (K) in muscles and stained with antibodies to HRP (magenta) and α-spectrin (cyan).

(L) Quantification of ghost boutons.

(M) Quantification of α-spectrin fluorescence.

(N–P) Quantification of lines crossed (N), peristaltic waves (O), and head sweeps (P).

For all experiments, data = mean ± SEM with significance calculated by ANOVA followed by Tukey's test for multiple comparisons. For (B)–(M), n ≥ 8 larvae, 16 NMJs; for (N)–(P), n ≥ 36 larvae. **p < 0.01, ***p < 0.001, n.s. = not significant. Scale bars, 10 μm, 5 μm (insets).

et al., 2014; Georgakopoulos et al., 1999, 2006; Inoue et al., 2009). We next used rat cortical neurons to determine if γ-secretase similarly promoted dendritic spine morphogenesis from filopodia to mushroom-headed spines, a process linked to maturation (Rochefort and Konnerth, 2012). To perturb γ-secretase in cortical neurons, we again used L685,458 (Figures S4A–S4D) to block y-secretase activity; we cultured rat cortical neurons in the presence or absence of L685,458 and assayed dendritic spine density and subtype after 21 days *in vitro*. L685,458 application modestly reduced spine density (Figures S7M–S7Q) but significantly altered spine subtype. In control and drug-treated samples, we observed three spine classes: stubby, thin filopodia, and mushroom-headed. In L685,458-treated samples, there were significantly fewer mature mushroom-headed spines with a concomitant increase in thin filopodia (Figure S7R), suggesting impaired maturation. Thus, our findings suggest that perturbing γ-secretase activity impairs dendritic and synaptic development at vertebrate central synapses.

Please cite this article in press as: Restrepo et al., γ-secretase promotes *Drosophila* postsynaptic development through the cleavage of a Wnt receptor, Developmental Cell (2022), https://doi.org/10.1016/j.devcel.2022.05.006

CellPress
OPEN ACCESS

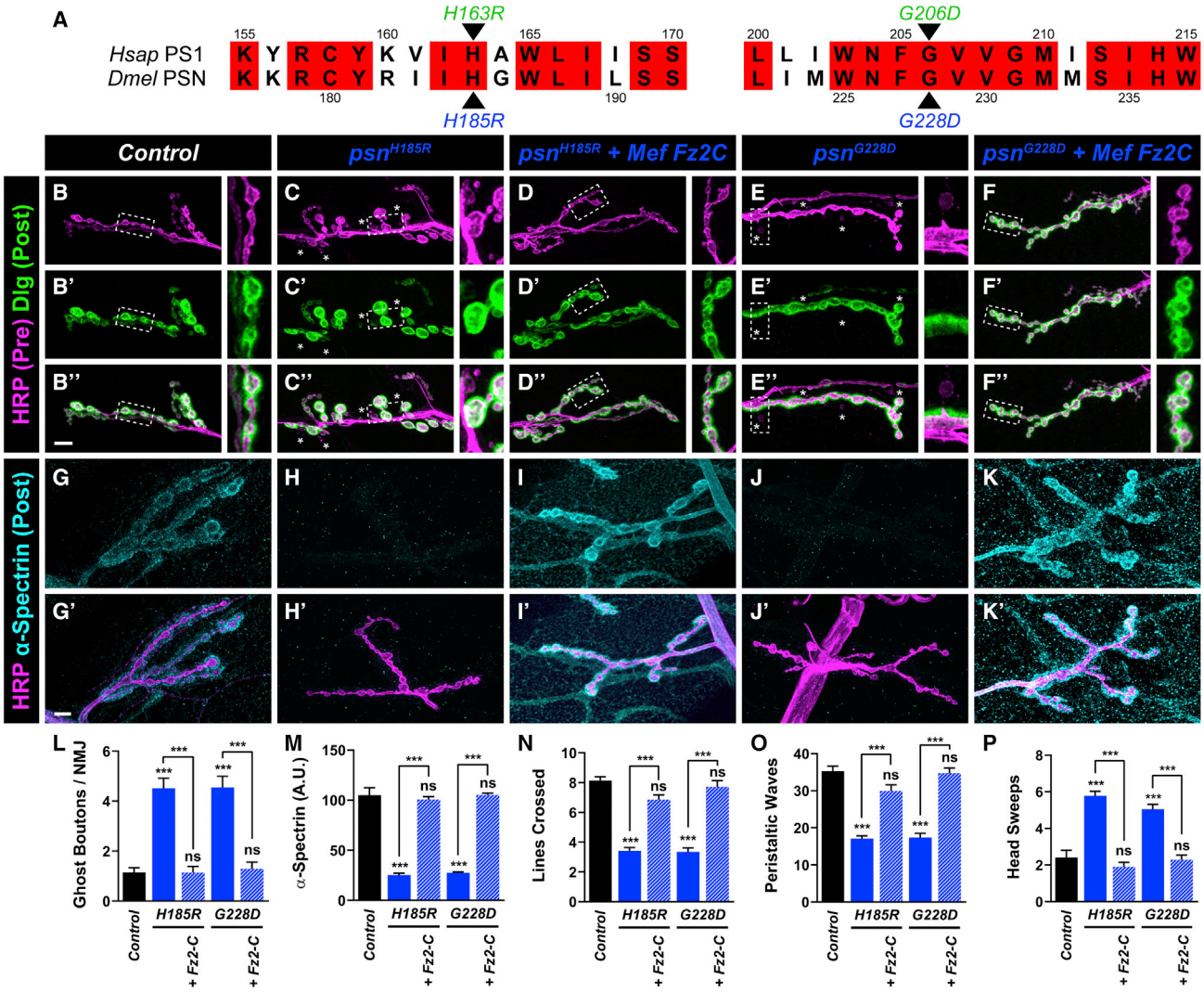

Figure 7. *PS1* mutations associated with early-onset Alzheimer's disease (EOAD) display defects in postsynaptic development and maturation and are suppressed by restoring nuclear Fz2-C

(A) Local sequence alignment of human PS1 (*Hsap*) and *Drosophila* Psn (*Dmel*). Conserved residues are in red. Human EOAD mutations (green) are shown with the corresponding *Drosophila* mutation (blue).

(B–F) Representative images of genotypes stained with antibodies to HRP (magenta) and Dlg (green). Asterisks indicate ghost boutons; insets represent high magnification (dashes).

(G–K) Representative images of *psn* EOAD alleles stained with antibodies to HRP (magenta) and α-spectrin (cyan).

(L) Quantification of ghost boutons.

(M) Quantification of α-spectrin fluorescence.

(N–P) Quantification of lines crossed (N), peristaltic waves (O), and head sweeps (P).

For all experiments, data = mean ± SEM with significance calculated by ANOVA followed by Tukey's test for multiple comparisons. In all, n ≥ 8 larvae, 16 NMJs. ***p < 0.001. Scale bars, 10 μm, 5 μm (inserts).

Patient *presenilin* mutations associated with Alzheimer's disease produce postsynaptic maturation defects

Missense mutations in *presenilin* underlie early-onset familial AD (Rogaev et al., 1995; Sherrington et al., 1995). Our discovery of a role for *psn* in promoting postsynaptic development and maturation motivated a translational question: do human *PSEN1* mutations linked to AD (De Strooper et al., 2012) also influence postsynaptic maturation? To address this question without overexpression models of disease-causing *psn* alleles, we used CRISPR-Cas9 editing (Bier et al., 2018) to make *Drosophila* lines with mutations in the endogenous *psn* locus that are equivalent to known human mutations linked to early-onset AD (EOAD). We compared human *PSEN1* and *Drosophila psn* and found that 27 of 36 mutations found in EOAD families (Lanoiselée et al., 2017) were in conserved residues. We focused on two specific mutations with distinct pathology and early age of onset: H163R and G206D (Lanoiselée et al., 2017); these residues correspond to H185 and G228 (Figure 7A), respectively, in fly *psn*. We made two transgenic lines containing the H185R or

Please cite this article in press as: Restrepo et al., γ-secretase promotes *Drosophila* postsynaptic development through the cleavage of a Wnt receptor, Developmental Cell (2022), https://doi.org/10.1016/j.devcel.2022.05.006

the G228D mutation in *psn* and examined synaptic maturation and behavior. Both psn^{H185R} and psn^{G228D} mutants displayed a 4- to 5-fold increase in ghost boutons (Figures 7B, 7C, 7E, and 7I) and markedly reduced α-spectrin (Figures 7G, 7H, 7J, and 7M), indicating impaired maturation. Both alleles also showed impaired behavior coordination (Figures 7N and 7P), as evidenced by reduced motility, peristalsis, and increased head sweeps. Both mutants were phenotypically indistinguishable from null *psn* alleles, suggesting loss of function. To determine if the observed defects were the result of failed nuclear Fz2-C import / cleavage (as with *psn* and *nct*) and could thus be suppressed by restoring nuclear Fz2-C, we expressed myc-NLS-Fz2-C in psn^{H185R} and psn^{G228D} mutant muscles and assayed ghost boutons, α-spectrin, larval motility, peristalsis, and head sweeping. Muscle-specific Fz2-C expression suppressed all defects in psn^{H185R} and psn^{G228D} mutants (Figures 7D, 7F, 7I, and 7K–7P). This indicates that the postsynaptic maturation defects associated with EOAD-linked *psn* alleles are due to the loss of nuclear Fz2-C, and there is phenotypic and mechanistic overlap between null mutations in, and EOAD-linked alleles of, *psn*. As such, understanding the molecules that promote neurodevelopment (here, Psn) may offer insight into how the same machinery influences neurodegeneration.

DISCUSSION

Postsynaptic development and maturation enable the essential transition from nascent, unreliable synapse to robust connection capable of high-fidelity neurotransmission. In *Drosophila*, the Wg ligand promotes neurodevelopment by activating postsynaptic Fz2 receptors, but the precise downstream events utilized by Fz2 to influence events like synaptic maturation remained controversial and unclear. Here, we find an unexpected developmental role for postsynaptic γ-secretase in enabling Fz2-mediated postsynaptic development via receptor cleavage. This role is also perturbed by AD patient-derived *PSEN1* alleles in *Drosophila*, suggesting a link between AD and Wnts. These data first solve longstanding mysteries as to the significance of, and factors required for, Fz2 cleavage in postsynaptic maturation. Second, it suggests that proteolytic receptor cleavage may be a shared mechanism between developmental and degenerative processes, raising the possibility of a prior unappreciated neurodevelopmental component to AD.

Postsynaptic Frizzled2, γ-secretase, and NMJ synapse maturation in *Drosophila*

In the last 20 years, work at the *Drosophila* NMJ revealed the importance of Wnts in regulating synaptic function and development through Fz2 and multiple downstream pathways (Chou et al., 2020; Harris and Littleton, 2015). The roles of each downstream pathway, however, remained unclear. In postsynaptic muscles, Fz2 signals via a FNI pathway resulting in nuclear import of cleaved Fz2 receptor (Mathew et al., 2005; Mosca and Schwarz, 2010a; Speese et al., 2012). Three major questions about FNI remained unanswered: (1) what is its physiological significance, (2) how does the Fz2 cleavage site lend to its physiological role, and (3) what protease is necessary for Fz2 cleavage to promotes this physiological role? Our work addresses each question, highlighting a role for FNI in postsynaptic development, the function of the cleavage site in synaptic maturation, and identifying γ-secretase as being required for Fz2 cleavage.

First, we show that postsynaptic Fz2 cleavage (and not canonical Wnt signaling) specifically promotes postsynaptic maturation (Figure 1). This does not preclude a postsynaptic Fz2 function in presynaptic growth and active zone establishment (Budnik and Salinas, 2011). Instead, postsynaptic Fz2 may promote growth via canonical pathways (Miech et al., 2008); this will be an important area for future study. Second, our identification of γ-secretase in promoting Fz2 cleavage (Figure 5) is critical to understand downstream Fz2 pathways and begins to answer longstanding questions in synaptic neurodevelopment and postsynaptic maturation. As the developmental defects in γ-secretase mutants are suppressed by activating the postsynaptic FNI pathway, this indicates that the relevant cleavage target in maturation is Fz2. As maturation defects underlie neurodevelopmental disorders (Zoghbi and Bear, 2012), further understanding the relevant machinery that promotes maturation can inform our grasp of neurodevelopment disease progression.

A conserved role for γ-secretase in synaptic development and maturation

Maturation of *Drosophila* central (Figure S7) and NMJ (Figures 4 and S2) synapses and mammalian dendritic spines (Figure S7) all require γ-secretase. γ-secretase promotes axon guidance and early synaptic development (Barão et al., 2015; Inoue et al., 2009; Javier-Torrent et al., 2019; Liu et al., 2018; Neuhaus-Follini and Bashaw, 2015; Peixoto et al., 2012; Sachse et al., 2019; Suzuki et al., 2012), but its role in synaptic maturation is largely unknown. Our data suggest γ-secretase-dependent cleavage and translocation of signaling proteins may be a fundamental feature of postsynaptic development (Liu et al., 2018; Nagappan-Chettiar et al., 2017; Toth et al., 2013). Indeed, blocking Presenilin::Syt I interaction modestly reduces spine density and mature spines (Zoltowska et al., 2017). This is consistent with our data, although the more general blockade of γ-secretase function has a larger effect on spine maturation. The mechanism remains unclear as γ-secretase modulates multiple downstream pathways, including Wnts (Barthet et al., 2018; Lee et al., 2014; Tabuchi et al., 2009; Zhang et al., 2009; Zoltowska et al., 2017). More work will be needed to determine if Wnt signaling is conserved in downstream signaling for synaptic maturation across evolution. In vertebrates, Fz5 and Fz8 are homologous to *Drosophila* Fz2 and contain the same consensus cleavage site (Mathew et al., 2005). Fz8 is expressed in the nervous system (Gong et al., 2016; Liu et al., 2012; Rawal et al., 2006), but its neuronal function and cleavage status remain unknown. Intriguingly, recent work showed that Fz5 can be cleaved in motor neuron-like NSC-34 cells (Kim et al., 2021). As Fz5 promotes activity-dependent synaptogenesis (Sahores et al., 2010) and neuronal survival (Liu et al., 2008), these data raise a tantalizing prospect that the γ-secretase / Wnt / Fz pathway is conserved in mammalian synaptic development.

Shared elements of postsynaptic development and neurodegenerative disease

Identifying a role for γ-secretase and its mechanistic basis in neurodevelopment offers insight into the potential function of γ-secretase in disease. *PSEN1* mutations are the most widely known genetic cause of EOAD (Lanoiselée et al., 2017), but we

Please cite this article in press as: Restrepo et al., γ-secretase promotes *Drosophila* postsynaptic development through the cleavage of a Wnt receptor, Developmental Cell (2022), https://doi.org/10.1016/j.devcel.2022.05.006

lack thorough understanding of this genetic link. Our data indicate that neurodevelopmental and neurodegenerative mechanisms may be united by a shared requirement for γ-secretase-dependent receptor processing. In AD, this adds a layer of connection between neurodevelopment and neurodegeneration via synapse-to-nucleus communication. In our model (Figure 6), γ-secretase cleavage enables Fz2-C generation and transition from synapse to nucleus (Mathew et al., 2005; Speese et al., 2012). In AD, the synapse-to-nucleus signals AIDA-1, ATF4, and CRTC1 (that are protein partners of cleaved receptor products) are also altered (Marcello et al., 2018) and blocking the synapse-to-nucleus translocation of Jacob, a protein that couples activity to CREB signaling, suppresses pathogenic Aβ-induced impairments (Gomes et al., 2014; Rönicke et al., 2011). We observed neurodevelopmental defects in EOAD mutations indistinguishable from loss-of-function mutants that could be suppressed by restoring nuclear Fz2-C (Figure 7). It will be important for future study to determine the intersection of proteolytic processing, synapse-to-nucleus signaling, and Wnts on AD (Tapia-Rojas and Inestrosa, 2018). Our data raise a tantalizing possibility of connecting AD to a previously unappreciated neurodevelopmental process, which can potentially provide earlier hallmarks to assess disease progression and inform therapeutic strategies to ameliorate disease states.

A prevailing mystery surrounding neurodegenerative diseases involves its onset. Although patients carry gene mutations all their lives, why do these disorders manifest later in life? A further challenge is to identify the earliest changes resulting from neurodegenerative disease gene mutations to better understand if symptoms are causative or correlative. The presence of synaptic maturation defects presents a hypothesis: if neurodegenerative disease risk genes are involved in synaptic maturation, the first reflection of mutations in those genes may be immature synapses that still function but lack the longevity of mature synapses. In advanced age, synapses constructed incorrectly during development may be the first to fail, leading to degeneration. AD models show reductions in postsynaptic proteins that precede neurodegeneration (Lleó et al., 2019). Further, growing evidence suggests that neurodegenerative diseases have synaptopathic origins (Taoufik et al., 2018) and early developmental defects (Huntley and Benson, 2020). It is further intriguing that molecules which influence synaptogenesis, like Ephs, are modified by γ-secretase (Sheffler-Collins and Dalva, 2012), potentially underlying further connection. Postsynaptic development and maturation may provide a unique angle to consider neurodegeneration, leading to earlier detection. With γ-secretase, maturation defects are suppressed by activating the downstream pathway (Figures 6 and 7); our data suggests analogous approaches may have clinical relevance. Whether synaptic NMJ phenotypes indicate a preclinical phenotype in disease models is an open question but examining postsynaptic maturation provides an opportunity to study shared mechanisms of neurodegenerative diseases, inform strategies to combat disease, and better understand neurodevelopment.

Limitations of the study: Fz2 receptors as γ-secretase cleavage substrates

Our data indicates that γ-secretase activity is required for Fz2 cleavage. First, γ-secretase and Fz2 localize close enough for interaction (Figures 5 and S5). Second, Fz2 and γ-secretase co-localize in the same subcellular compartments and traffic similarly (Figure S5). Third, our structural model predicts that the cleavage site embeds in the membrane (Figure S6), keeping it within the "lid" distance (Xie et al., 2014) to be recognized as a cleavage site. Moving the cleavage site so it no longer abuts the membrane prevents the cleavage-dependent functions of Fz2 (Figure S6). The most parsimonious interpretation supports Fz2 cleavage by γ-secretase. However, it is important to note that the data do not conclusively imply a direct cleavage event. Fz2 is not a canonical γ-secretase substrate for several reasons. First, γ-secretase typically cleaves single pass transmembrane proteins (Güner and Lichtenthaler, 2020); Fz2 is a 7-pass transmembrane domain atypical G-protein coupled receptor (GPCR). This is not a requisite, however, as multipass transmembrane proteins like neuregulin-1 can be cleaved by γ-secretase (Fleck et al., 2016). Second, γ-secretase typically cleaves in a processive fashion: the substrate ectodomain is first shed via an ADAM (a disintegrin and metallprotease) enzyme or β-secretase (Wolfe, 2009), after which γ-secretase cleavage releases the substrate intracellular domain. There is no evidence that Fz2 undergoes ectodomain shedding (Kim et al., 2021; Mathew et al., 2005) and the receptor lacks consensus N-terminal cleavage sites. Third, γ-secretase typically cleaves in the plane of the membrane (Li et al., 2016). The Fz2 cleavage site is cytosolic, although predicted to juxtapose the membrane (Figure S6). Recent years, however, identified noncanonical substrates that serve as exceptions to this rule (Güner and Lichtenthaler, 2020).

Our data suggest that GPCRs may be atypical γ-secretase cleavage targets. This broadens the potential repertoire of γ-secretase, underscoring its importance in diverse processes. However, we cannot rule out alternate interpretations where Fz2 cleavage requires ectodomain shedding or occurs via successive events (Fleck et al., 2016). In the latter, Fz2 would still be a direct target of γ-secretase that follows a preceding event. Also, γ-secretase may cleave a secondary target that allows Fz2 to be cleaved. In all cases, the activity of γ-secretase is still required for Fz2 cleavage. Future study in a cell-free system (Bai et al., 2015; Stempfle et al., 2010) will be required for formal proof. Regardless, the complete suppression of the γ-secretase developmental phenotypes by nuclear Fz2-C expression (Figures 6 and 7) indicates the most relevant cellular substrate in promoting postsynaptic development and maturation via γ-secretase is cleaved Fz2-C.

STAR★METHODS

Detailed methods are provided in the online version of this paper and include the following:

- KEY RESOURCES TABLE
- RESOURCE AVAILABILITY
  - Lead contact
  - Materials availability
  - Data and code availability
- EXPERIMENTAL MODEL AND SUBJECT DETAILS
  - Drosophila stocks and transgenic strains
  - Construction of psn^{H185R} and psn^{G228D}
  - Cloning of Fz2 constructs and transgenic line production

SUPPLEMENTAL INFORMATION

Supplemental information can be found online at https://doi.org/10.1016/j.devcel.2022.05.006.

ACKNOWLEDGMENTS

We thank Shernaz Bamji, Matthew Dalva, Kristen Davis, Chris Doe, Jesse Humenik, Irwin Levitan, Craig Montell, Joaquin Navajas Acedo, and S. Zosimus for insightful comments on the manuscript. We especially thank Engin Özkan for his curiosity and guidance in structural modeling. We deeply appreciate the gifts of reagents from Yashi Ahmed, Jeffrey Axelrod, Vivian Budnik, Matthew Dalva, Mark Fortini, Alison Goate, Le Ma, Kate O'Connor-Giles, Tom Schwarz, and Gary Struhl. Stocks obtained from the Bloomington Drosophila Stock Center (NIH P40OD018537) were also used in this study. T.J.M. would like to thank Tom Schwarz, in whose lab his fascination with Fz2-C began. This work was supported by US National Institute of Health grants R01-NS110907 and R00-DC013059 (to T.J.M.) and F31-NS120718 (to A.T.D.). Work in the T.J.M. Lab is supported by the Alfred P. Sloan Foundation, Whitehall Foundation, Jefferson Dean's Transformational Science Award, Jefferson Synaptic Biology Center, Commonwealth Universal Research Enhancement of the Pennsylvania Department of Health, and TJU start-up funds.

AUTHOR CONTRIBUTIONS

L.J.R. and T.J.M. designed the project. L.J.R., A.T.D., E.R.M., M.A.A., J.C.D., S.R.T., H.F., and T.J.M. performed experiments. M.J.P. and T.J.M. produced reagents. L.J.R., A.T.D., E.R.M., M.A.A., and T.J.M. analyzed the data. L.J.R. and T.J.M. wrote the manuscript. L.J.R., A.T.D., E.R.M., M.A.A., J.C.D., M.J.P., and T.J.M. edited the manuscript.

DECLARATION OF INTERESTS

The authors declare no competing interests.

INCLUSION AND DIVERSITY

We worked to ensure sex balance in the selection of non-human subjects. One or more of the authors of this paper self-identifies as an underrepresented ethnic minority in science. One or more of the authors of this paper self-identifies as a member of the LGBTQ+ community. One or more of the authors of this paper self-identifies as living with a disability. While citing references scientifically relevant for this work, we also actively worked to promote gender balance in our reference list.

Received: October 4, 2021
Revised: April 6, 2022
Accepted: May 10, 2022
Published: June 1, 2022

REFERENCES

Allan, D.W., St Pierre, S.E., Miguel-Aliaga, I., and Thor, S. (2003). Specification of neuropeptide cell identity by the integration of retrograde BMP signaling and a combinatorial transcription factor code. Cell *113*, 73–86.

Artavanis-Tsakonas, S. (2004). Accessing the Exelixis collection. Nat. Genet. *36*, 207.

Ashley, J., Cordy, B., Lucia, D., Fradkin, L.G., Budnik, V., and Thomson, T. (2018). Retrovirus-like gag protein Arc1 binds RNA and traffics across synaptic boutons. Cell *172*, 262–274.e11.

Ataman, B., Ashley, J., Gorczyca, D., Gorczyca, M., Mathew, D., Wichmann, C., Sigrist, S.J., and Budnik, V. (2006). Nuclear trafficking of *Drosophila* Frizzled-2 during synapse development requires the PDZ protein dGRIP. Proc. Natl. Acad. Sci. USA *103*, 7841–7846.

Ataman, B., Ashley, J., Gorczyca, M., Ramachandran, P., Fouquet, W., Sigrist, S.J., and Budnik, V. (2008). Rapid activity-dependent modifications in synaptic structure and function require bidirectional wnt signaling. Neuron *57*, 705–718.

Axelrod, J.D., Miller, J.R., Shulman, J.M., Moon, R.T., and Perrimon, N. (1998). Differential recruitment of dishevelled provides signaling specificity in the planar cell polarity and Wingless signaling pathways. Genes Dev. *12*, 2610–2622.

Bai, X.C., Yan, C., Yang, G., Lu, P., Ma, D., Sun, L., Zhou, R., Scheres, S.H.W., and Shi, Y. (2015). An atomic structure of human γ-secretase. Nature *525*, 212–217.

Barão, S., Gärtner, A., Leyva-Díaz, E., Demyanenko, G., Munck, S., Vanhoutvin, T., Zhou, L., Schachner, M., López-Bendito, G., Maness, P.F., et al. (2015). Antagonistic effects of BACE1 and APH1B-γ-Secretase control axonal guidance by regulating growth cone collapse. Cell Rep. *12*, 1367–1376.

Barnat, M., Capizzi, M., Aparicio, E., Boluda, S., Wennagel, D., Kacher, R., Kassem, R., Lenoir, S., Agasse, F., Braz, B.Y., et al. (2020). Huntington's disease alters human neurodevelopment. Science *369*, 787–793.

Barthet, G., Dunys, J., Shao, Z., Xuan, Z., Ren, Y., Xu, J., Arbez, N., Mauger, G., Bruban, J., Georgakopoulos, A., et al. (2013). Presenilin mediates neuroprotective functions of ephrinB and brain-derived neurotrophic factor and regulates ligand-induced internalization and metabolism of EphB2 and TrkB receptors. Neurobiol. Aging *34*, 499–510.

Barthet, G., Jordà-Siquier, T., Rumi-Masante, J., Bernadou, F., Müller, U., and Mulle, C. (2018). Presenilin-mediated cleavage of APP regulates synaptotagmin-7 and presynaptic plasticity. Nat. Commun. *9*, 4780.

Bier, E., Harrison, M.M., O'Connor-Giles, K.M., and Wildonger, J. (2018). Advances in engineering the fly genome with the CRISPR-Cas system. Genetics *208*, 1–18.

Blunk, A.D., Akbergenova, Y., Cho, R.W., Lee, J., Walldorf, U., Xu, K., Zhong, G., Zhuang, X., and Littleton, J.T. (2014). Postsynaptic actin regulates active zone spacing and glutamate receptor apposition at the *Drosophila* neuromuscular junction. Mol. Cell. Neurosci. *61*, 241–254.

Boll, W., and Noll, M. (2002). The *Drosophila* Pox neuro gene: control of male courtship behavior and fertility as revealed by a complete dissection of all enhancers. Development *129*, 5667–5681.

Boutros, M., Mihaly, J., Bouwmeester, T., and Mlodzik, M. (2000). Signaling specificity by frizzled receptors in *Drosophila*. Science *288*, 1825–1828.

Budnik, V., Koh, Y.H., Guan, B., Hartmann, B., Hough, C., Woods, D., and Gorczyca, M. (1996). Regulation of synapse structure and function by the *Drosophila* tumor suppressor gene dlg. Neuron *17*, 627–640.

Budnik, V., and Salinas, P.C. (2011). Wnt signaling during synaptic development and plasticity. Curr. Opin. Neurobiol. *21*, 151–159.

Byers, T.J., Dubreuil, R., Branton, D., Kiehart, D.P., and Goldstein, L.S.B. (1987). *Drosophila* spectrin. II. Conserved features of the alpha-subunit are revealed by analysis of cDNA clones and fusion proteins. J. Cell Biol. *105*, 2103–2110.

Charng, W.L., Yamamoto, S., and Bellen, H.J. (2014). Shared mechanisms between *Drosophila* peripheral nervous system development and human neurodegenerative diseases. Curr. Opin. Neurobiol. *27*, 158–164.

Chen, C.M., and Struhl, G. (1999). Wingless transduction by the Frizzled and Frizzled2 proteins of *Drosophila*. Development *126*, 5441–5452.

Chia, P.H., Li, P., and Shen, K. (2013). Cell biology in neuroscience: cellular and molecular mechanisms underlying presynapse formation. J. Cell Biol. *203*, 11–22.

Chou, V.T., Johnson, S.A., and Van Vactor, D. (2020). Synapse development and maturation at the *Drosophila* neuromuscular junction. Neural Dev. *15*, 11.

Clark, M.Q., Zarin, A.A., Carreira-Rosario, A., and Doe, C.Q. (2018). Neural circuits driving larval locomotion in *Drosophila*. Neural Dev. *13*, 6.

Clement, J.P., Aceti, M., Creson, T.K., Ozkan, E.D., Shi, Y., Reish, N.J., Almonte, A.G., Miller, B.H., Wiltgen, B.J., Miller, C.A., et al. (2012). Pathogenic SYNGAP1 mutations impair cognitive development by disrupting maturation of dendritic spine synapses. Cell *151*, 709–723.

Collins, C.A., and DiAntonio, A. (2007). Synaptic development: insights from *Drosophila*. Curr. Opin. Neurobiol. *17*, 35–42.

De Bivort, B.L., Guo, H.F., and Zhong, Y. (2009). Notch Signaling is required for activity-dependent synaptic plasticity at the *Drosophila* neuromuscular junction. J. Neurogenet. *23*, 395–404.

De Strooper, B., Iwatsubo, T., and Wolfe, M.S. (2012). Presenilins and γ-secretase: structure, function, and role in Alzheimer disease. Cold Spring Harb. Perspect. Med. *2*, a006304.

Department of Biology University of Oregon (1974). *Drosophila* Information Service. Drosoph. Inf. Serv. *51*, 227.

Dietzl, G., Chen, D., Schnorrer, F., Su, K.C., Barinova, Y., Fellner, M., Gasser, B., Kinsey, K., Oppel, S., Scheiblauer, S., et al. (2007). A genome-wide transgenic RNAi library for conditional gene inactivation in *Drosophila*. Nature *448*, 151–156.

Eaton, B.A., and Davis, G.W. (2005). LIM kinase1 controls synaptic stability downstream of the type II BMP receptor. Neuron *47*, 695–708.

Fazzari, P., Snellinx, A., Sabanov, V., Ahmed, T., Serneels, L., Gartner, A., Shariati, S.A.M., Balschun, D., and De Strooper, B. (2014). Cell autonomous regulation of hippocampal circuitry via Aph1b-γ-secretase/neuregulin 1 signalling. eLife *3*, 1–16.

Fleck, D., Voss, M., Brankatschk, B., Giudici, C., Hampel, H., Schwenk, B., Edbauer, D., Fukumori, A., Steiner, H., Kremmer, E., et al. (2016). Proteolytic processing of neuregulin 1 type III by three intramembrane-cleaving proteases. J. Biol. Chem. *291*, 318–333.

Fouquet, W., Owald, D., Wichmann, C., Mertel, S., Depner, H., Dyba, M., Hallermann, S., Kittel, R.J., Eimer, S., and Sigrist, S.J. (2009). Maturation of active zone assembly by *Drosophila* Bruchpilot. J. Cell Biol. *186*, 129–145.

Fradkin, L.G., Garriga, G., Salinas, P.C., Thomas, J.B., Yu, X., and Zou, Y. (2005). Wnt signaling in neural circuit development. J. Neurosci. *25*, 10376–10378.

Fuentes-Medel, Y., Logan, M.A., Ashley, J., Ataman, B., Budnik, V., and Freeman, M.R. (2009). Glia and muscle sculpt neuromuscular arbors by engulfing destabilized synaptic boutons and shed presynaptic debris. PLoS Biol. *7*, e1000184.

Fushiki, A., Zwart, M.F., Kohsaka, H., Fetter, R.D., Cardona, A., and Nose, A. (2016). A circuit mechanism for the propagation of waves of muscle contraction in *Drosophila*. Elife *5*, 1–23.

Georgakopoulos, A., Litterst, C., Ghersi, E., Baki, L., Xu, C.J., Serban, G., and Robakis, N.K. (2006). Metalloproteinase/presenilin1 processing of ephrinB regulates EphB-induced Src phosphorylation and signaling. EMBO J. *25*, 1242–1252.

Georgakopoulos, A., Marambaud, P., Efthimiopoulos, S., Shioi, J., Cui, W., Li, H.C., Schütte, M., Gordon, R., Holstein, G.R., Martinelli, G., et al. (1999). Presenilin-1 forms complexes with the cadherin/catenin cell-cell adhesion system and is recruited to intercellular and synaptic contacts. Mol. Cell *4*, 893–902.

Gomes, G.M., Dalmolin, G.D., Bär, J., Karpova, A., Mello, C.F., Kreutz, M.R., and Rubin, M.A. (2014). Inhibition of the polyamine system counteracts β-amyloid peptide-induced memory impairment in mice: involvement of extrasynaptic NMDA receptors. PLoS One *9*, e99184.

Gong, G., Hu, L., Qin, F., Yin, L., Yi, X., Yuan, L., and Wu, W. (2016). Spinal WNT pathway contributes to remifentanil induced hyperalgesia through regulating fractalkine and CX3CR1 in rats. Neurosci. Lett. *633*, 21–27.

Gratz, S.J., Harrison, M.M., Wildonger, J., and O'Connor-Giles, K.M. (2015). Precise genome editing of *Drosophila* with CRISPR RNA- guided cas9. Methods Mol. Biol. *1311*, 335–348.

Güner, G., and Lichtenthaler, S.F. (2020). The substrate repertoire of γ-secretase/presenilin. Semin. Cell Dev. Biol. *105*, 27–42.

Harris, K.P., Akbergenova, Y., Cho, R.W., Baas-Thomas, M.S., and Littleton, J.T. (2016). Shank modulates postsynaptic wnt signaling to regulate synaptic development. J. Neurosci. *36*, 5820–5832.

Harris, K.P., and Littleton, J.T. (2015). Transmission, development, and plasticity of synapses. Genetics *201*, 345–375.

Higashi-Kovtun, M.E., Mosca, T.J., Dickman, D.K., Meinertzhagen, I.A., and Schwarz, T.L. (2010). Importin-β11 regulates synaptic phosphorylated mothers against decapentaplegic, and thereby influences synaptic development and function at the *Drosophila* neuromuscular junction. J. Neurosci. *30*, 5253–5268.

Hooks, B.M., and Chen, C. (2020). Circuitry underlying experience-dependent plasticity in the mouse visual system. Neuron *106*, 21–36.

Hoy, J.L., Haeger, P.A., Constable, J.R.L., Arias, R.J., McCallum, R., Kyweriga, M., Davis, L., Schnell, E., Wehr, M., Castillo, P.E., et al. (2013). Neuroligin1 drives synaptic and behavioral maturation through intracellular interactions. J. Neurosci. *33*, 9364–9384.

Hu, Y., Comjean, A., Roesel, C., Vinayagam, A., Flockhart, I., Zirin, J., Perkins, L., Perrimon, N., and Mohr, S.E. (2017). FlyRNAi.org - The database of the *Drosophila* RNAi screening center and transgenic RNAi project: 2017 update. Nucleic Acids Res. *45*, D672–D678.

Hu, Y., and Fortini, M.E. (2003). Different cofactor activities in γ-secretase assembly: evidence for a nicastrin – Aph-1 subcomplex. J. Cell Biol. *161*, 685–690.

Hu, Y., Ye, Y., and Fortini, M.E. (2002). Nicastrin is required for γ-secretase cleavage of the *Drosophila* Notch receptor. Dev. Cell *2*, 69–78.

Humberg, T.H., Bruegger, P., Afonso, B., Zlatic, M., Truman, J.W., Gershow, M., Samuel, A., and Sprecher, S.G. (2018). Dedicated photoreceptor pathways in *Drosophila* larvae mediate navigation by processing either spatial or temporal cues. Nat. Commun. *9*, 1260.

Huntley, G.W., and Benson, D.L. (2020). Origins of Parkinson's disease in brain development: insights From early and persistent effects of LRRK2-G2019S on striatal circuits. Front. Neurosci. *14*, 265.

Inoue, E., Deguchi-Tawarada, M., Togawa, A., Matsui, C., Arita, K., Katahira-Tayama, S., Sato, T., Yamauchi, E., Oda, Y., and Takai, Y. (2009). Synaptic activity prompts γ-secretase-mediated cleavage of EphA4 and dendritic spine formation. J. Cell Biol. *185*, 551–564.

Iwai, Y., Usui, T., Hirano, S., Steward, R., Takeichi, M., and Uemura, T. (1997). Axon patterning requires DN-cadherin, a novel neuronal adhesion receptor, in the *Drosophila* embryonic CNS. Neuron *19*, 77–89.

Javier-Torrent, M., Marco, S., Rocandio, D., Pons-Vizcarra, M., Janes, P.W., Lackmann, M., Egea, J., and Saura, C.A. (2019). Presenilin/γ-secretase-dependent epha3 processing mediates axon elongation through non-muscle myosin IIA. eLife *8*, 1–26.

Kamimura, K., Ueno, K., Nakagawa, J., Hamada, R., Saitoe, M., and Maeda, N. (2013). Perlecan regulates bidirectional Wnt signaling at the *Drosophila* neuromuscular junction. J. Cell Biol. *200*, 219–233.

Kane, E.A., Gershow, M., Afonso, B., Larderet, I., Klein, M., Carter, A.R., De Bivort, B.L., Sprecher, S.G., and Samuel, A.D.T. (2013). Sensorimotor structure of *Drosophila* larva phototaxis. Proc. Natl. Acad. Sci. USA *110*, E3868–E3877.

Kerr, K.S., Fuentes-Medel, Y., Brewer, C., Barria, R., Ashley, J., Abruzzi, K.C., Sheehan, A., Tasdemir-Yilmaz, O.E., Freeman, M.R., and Budnik, V. (2014). Glial wingless/wnt regulates glutamate receptor clustering and synaptic physiology at the *Drosophila* neuromuscular junction. J. Neurosci. *34*, 2910–2920.

Keshishian, H., Broadie, K., Chiba, A., and Bate, M. (1996). The *Drosophila* neuromuscular junction: a model system for studying synaptic development and function. Annu. Rev. Neurosci. *19*, 545–575.

Kim, J., Kim, S., Nahm, M., Li, T.-N., Lin, H.-C., Kim, Y.D., Lee, J., Yao, C.-K., and Lee, S. (2021). ALS2 regulates endosomal trafficking, postsynaptic development, and neuronal survival. J. Cell Biol. *220*, e202007112.

Knight, D., Iliadi, K., Charlton, M.P., Atwood, H.L., and Boulianne, G.L. (2007). Presynaptic plasticity and associative learning are impaired in a *Drosophila* presenilin null mutant. Dev. Neurobiol. *67*, 1598–1613.

Koh, Y.H., Popova, E., Thomas, U., Griffith, L.C., and Budnik, V. (1999). Regulation of DLG localization at synapses by CaMKII-dependent phosphorylation. Cell *98*, 353–363.

Korkut, C., Ataman, B., Ramachandran, P., Ashley, J., Barria, R., Gherbesi, N., and Budnik, V. (2009). Trans-synaptic transmission of vesicular wnt signals through Evi/Wntless. Cell *139*, 393–404.

Krogh, A., Larsson, B., Von Heijne, G., and Sonnhammer, E.L.L. (2001). Predicting transmembrane protein topology with a hidden Markov model: application to complete genomes. J. Mol. Biol. *305*, 567–580.

Kurtovic, A., Widmer, A., and Dickson, B.J. (2007). A single class of olfactory neurons mediates behavioural responses to a *Drosophila* sex pheromone. Nature *446*, 542–546.

Laissue, P.P., Reiter, C., Hiesinger, P.R., Halter, S., Fischbach, K.F., and Stocker, R.F. (1999). Three-dimensional reconstruction of the antennal lobe in *Drosophila* melanogaster. J. Comp. Neurol. *405*, 543–552.

Lanoiselée, H.M., Nicolas, G., Wallon, D., Rovelet-Lecrux, A., Lacour, M., Rousseau, S., Richard, A.C., Pasquier, F., Rollin-Sillaire, A., Martinaud, O., et al. (2017). APP, PSEN1, and PSEN2 mutations in early-onset Alzheimer disease: a genetic screening study of familial and sporadic cases. PLoS Med. *14*, e1002270.

Lathia, J.D., Mattson, M.P., and Cheng, A. (2008). Notch: from neural development to neurological disorders. J. Neurochem. *107*, 1471–1481.

Lee, S.H., Sharma, M., Südhof, T.C., and Shen, J. (2014). Synaptic function of nicastrin in hippocampal neurons. Proc. Natl. Acad. Sci. USA *111*, 8973–8978.

Li, N., Liu, K., Qiu, Y., Ren, Z., Dai, R., Deng, Y., and Qing, H. (2016). Effect of presenilin mutations on APP cleavage; insights into the pathogenesis of FAD. Front. Aging Neurosci. *8*, 51.

Lilly, B., Zhao, B., Ranganayakulu, G., Paterson, B.M., Schulz, R.A., and Olson, E.N. (1995). Requirement of MADS domain transcription factor D-MEF2 for muscle formation in *Drosophila*. Science *267*, 688–693.

Lin, D.M., and Goodman, C.S. (1994). Ectopic and increased expression of fasciclin II alters motoneuron growth cone guidance. Neuron *13*, 507–523.

Liu, C., Bakeri, H., Li, T., and Swaroop, A. (2012). Regulation of retinal progenitor expansion by Frizzled receptors: implications for microphthalmia and retinal coloboma. Hum. Mol. Genet. *21*, 1848–1860.

Liu, C., Wang, Y., Smallwood, P.M., and Nathans, J. (2008). An essential role for Frizzled5 in neuronal survival in the parafascicular nucleus of the thalamus. J. Neurosci. *28*, 5641–5653.

Liu, Z., Thakar, A., Santoro, S.W., and Pratt, K.G. (2018). Presenilin regulates retinotectal synapse formation through EphB2 receptor processing. Dev. Neurobiol. *78*, 1171–1190.

Lleó, A., Núñez-Llaves, R., Alcolea, D., Chiva, C., Balateu-Paños, D., Colom-Cadena, M., Gomez-Giro, G., Muñoz, L., Querol-Vilaseca, M., Pegueroles, J., et al. (2019). Changes in synaptic proteins precede neurodegeneration markers in preclinical Alzheimer's disease cerebrospinal fluid. Mol. Cell. Proteomics *18*, 546–560.

Lnenicka, G.A., and Keshishian, H. (2000). Identified motor terminals in *Drosophila* larvae show distinct differences in morphology and physiology. J. Neurobiol. *43*, 186–197.

Lnenicka, G.A., Spencer, G.M., and Keshishian, H. (2003). Effect of reduced impulse activity on the development of identified motor terminals in *Drosophila* larvae. J. Neurobiol. *54*, 337–345.

Lorenzen, J.A., Baker, S.E., Denhez, F., Melnick, M.B., Brower, D.L., and Perkins, L.A. (2001). Nuclear import of activated D-ERK by DIM-7, an importin family member encoded by the gene moleskin. Development *128*, 1403–1414.

Lukinova, N.I., Roussakova, V.V., and Fortini, M.E. (1999). Genetic characterization of cytological region 77A-D harboring the presenilin gene of *Drosophila melanogaster*. Genetics *153*, 1789–1797.

Luo, L., Liao, Y.J., Jan, L.Y., and Jan, Y.N. (1994). Distinct morphogenetic functions of similar small GTPases: *Drosophila* Drac1 is involved in axonal outgrowth and myoblast fusion. Genes Dev. *8*, 1787–1802.

Luo, L., Tully, T., and White, K. (1992). Human amyloid precursor protein ameliorates behavioral deficit of flies deleted for Appl gene. Neuron *9*, 595–605.

Mackler, J.M., Drummond, J.A., Loewen, C.A., Robinson, I.M., and Reist, N.E. (2002). The C2B Ca^{2+}-binding motif of synaptotagmin is required for synaptic transmission *in vivo*. Nature *418*, 340–344.

Mahoney, M.B., Parks, A.L., Ruddy, D.A., Tiong, S.Y.K., Esengil, H., Phan, A.C., Philandrinos, P., Winter, C.G., Chatterjee, R., Huppert, K., et al. (2006). Presenilin-based genetic screens in *Drosophila melanogaster* identify novel Notch pathway modifiers. Genetics *172*, 2309–2324.

Marcello, E., Di Luca, M., and Gardoni, F. (2018). Synapse-to-nucleus communication: from developmental disorders to Alzheimer's disease. Curr. Opin. Neurobiol. *48*, 160–166.

Marrus, S.B., Portman, S.L., Allen, M.J., Moffat, K.G., and DiAntonio, A. (2004). Differential localization of glutamate receptor subunits at the drosophila neuromuscular junction. J. Neurosci. *24*, 1406–1415.

Mathew, D., Ataman, B., Chen, J., Zhang, Y., Cumberledge, S., and Budnik, V. (2005). Wingless signaling at synapses is through cleavage and nuclear import of receptor DFrizzled2. Science *310*, 1344–1347.

Miech, C., Pauer, H.U., He, X., and Schwarz, T.L. (2008). Presynaptic local signaling by a canonical wingless pathway regulates development of the Drosophila neuromuscular junction. J. Neurosci. *28*, 10875–10884.

Mosca, T.J., Hong, W., Dani, V.S., Favaloro, V., and Luo, L. (2012). Trans-synaptic teneurin signalling in neuromuscular synapse organization and target choice. Nature *484*, 237–241.

Mosca, T.J., Luginbuhl, D.J., Wang, I.E., and Luo, L. (2017). Presynaptic LRP4 promotes synapse number and function of excitatory CNS neurons. Elife *6*, 115907.

Mosca, T.J., and Luo, L. (2014). Synaptic organization of the Drosophila antennal lobe and its regulation by the teneurins. Elife *3*, e03726.

Mosca, T.J., and Schwarz, T.L. (2010a). The nuclear import of Frizzled2-C by Importins-β 211 and Î ±2 promotes postsynaptic development. Nat. Neurosci. *13*, 935–943.

Mosca, T.J., and Schwarz, T.L. (2010b). Drosophila importin-α2 is involved in synapse, axon and muscle development. PLoS One *5*, e15223.

Nagappan-Chettiar, S., Johnson-Venkatesh, E.M., and Umemori, H. (2017). Activity-dependent proteolytic cleavage of cell adhesion molecules regulates excitatory synaptic development and function. Neurosci. Res. *116*, 60–69.

Nalivaeva, N.N., and Turner, A.J. (2013). Neprilysin. In Handbook of Proteolytic Enzymes (Elsevier), pp. 612–619.

Neuhaus-Follini, A., and Bashaw, G.J. (2015). The intracellular domain of the frazzled/DCC receptor is a transcription factor required for commissural axon guidance. Neuron *87*, 751–763.

Nowotny, P., Gorski, S.M., Han, S.W., Philips, K., Ray, W.J., Nowotny, V., Jones, C.J., Clark, R.F., Cagan, R.L., and Goate, A.M. (2000). Posttranslational modification and plasma membrane localization of the *Drosophila melanogaster* presenilin. Mol. Cell. Neurosci. *15*, 88–98.

Oliva, C.A., Montecinos-Oliva, C., and Inestrosa, N.C. (2018). Wnt Signaling in the Central Nervous System: New Insights in Health and Disease (Elsevier Inc.).

Packard, M., Koo, E.S., Gorczyca, M., Sharpe, J., Cumberledge, S., and Budnik, V. (2002). The Drosophila Wnt, wingless, provides an essential signal for pre- and postsynaptic differentiation. Cell *111*, 319–330.

Pai, L.M., Orsulic, S., Bejsovec, A., and Peifer, M. (1997). Negative regulation of Armadillo, a Wingless effector in Drosophila. Development *124*, 2255–2266.

Pan, D., and Rubin, G.M. (1997). Kuzbanian controls proteolytic processing of Notch and mediates lateral inhibition during Drosophila and vertebrate neurogenesis. Cell *90*, 271–280.

Parnas, D., Haghighi, A.P., Fetter, R.D., Kim, S.W., and Goodman, C.S. (2001). Regulation of postsynaptic structure and protein localization by the Rho-type guanine nucleotide exchange factor dPix. Neuron *32*, 415–424.

Peixoto, R.T., Kunz, P.A., Kwon, H., Mabb, A.M., Sabatini, B.L., Philpot, B.D., and Ehlers, M.D. (2012). Transsynaptic signaling by activity-dependent cleavage of Neuroligin-1. Neuron *76*, 396–409.

Piccioli, Z.D., and Littleton, J.T. (2014). Retrograde BMP signaling modulates rapid activity-dependent synaptic growth via presynaptic lim kinase regulation of cofilin. J. Neurosci. *34*, 4371–4381.

Piddini, E., Marshall, F., Dubois, L., Hirst, E., and Vincent, J.P. (2005). Arrow (LRP6) and Frizzled2 cooperate to degrade Wingless in Drosophila imaginal discs. Development *132*, 5479–5489.

Pielage, J., Cheng, L., Fetter, R.D., Carlton, P.M., Sedat, J.W., and Davis, G.W. (2008). A presynaptic giant ankyrin stabilizes the NMJ through regulation of presynaptic microtubules and transsynaptic cell adhesion. Neuron *58*, 195–209.

Pielage, J., Fetter, R.D., and Davis, G.W. (2005). Presynaptic spectrin is essential for synapse stabilization. Curr. Biol. *15*, 918–928.

Rasse, T.M., Fouquet, W., Schmid, A., Kittel, R.J., Mertel, S., Sigrist, C.B., Schmidt, M., Guzman, A., Merino, C., Qin, G., et al. (2005). Glutamate receptor dynamics organizing synapse formation *in vivo*. Nat. Neurosci. *8*, 898–905.

Rawal, N., Castelo-Branco, G., Sousa, K.M., Kele, J., Kobayashi, K., Okano, H., and Arenas, E. (2006). Dynamic temporal and cell type-specific expression of Wnt signaling components in the developing midbrain. Exp. Cell Res. *312*, 1626–1636.

Reichsman, F., Smith, L., and Cumberledge, S. (1996). Glycosaminoglycans can modulate extracellular localization of the wingless protein and promote signal transduction. J. Cell Biol. *135*, 819–827.

Riemer, D., Stuurman, N., Berrios, M., Hunter, C., Fisher, P.A., and Weber, K. (1995). Expression of drosophila lamin C is developmentally regulated: analogies with vertebrate A-type lamins. J. Cell Sci. *108*, 3189–3198.

Rochefort, N.L., and Konnerth, A. (2012). Dendritic spines: from structure to *in vivo* function. EMBO Rep. *13*, 699–708.

Rogaev, E.I., Sherrington, R., Rogaeva, E.A., Levesque, G., Ikeda, M., Liang, Y., Chi, H., Lin, C., Holman, K., and Tsuda, T. (1995). Familial Alzheimer's disease in kindreds with missense mutations in a gene on chromosome 1 related to the Alzheimer's disease type 3 gene. Nature *376*, 775–778.

Rönicke, R., Mikhaylova, M., Rönicke, S., Meinhardt, J., Schröder, U.H., Fändrich, M., Reiser, G., Kreutz, M.R., and Reymann, K.G. (2011). Early neuronal dysfunction by amyloid β oligomers depends on activation of NR2B-containing NMDA receptors. Neurobiol. Aging *32*, 2219–2228.

Sachse, S.M., Lievens, S., Ribeiro, L.F., Dascenco, D., Masschaele, D., Horré, K., Misbaer, A., Vanderroost, N., De Smet, A.S., Salta, E., et al. (2019). Nuclear import of the DSCAM-cytoplasmic domain drives signaling capable of inhibiting synapse formation. EMBO J. *38*, 1–19.

Sahores, M., Gibb, A., and Salinas, P.C. (2010). Frizzled-5, a receptor for the synaptic organizer Wnt7a, regulates activity-mediated synaptogenesis. Development *137*, 2215–2225.

Salinas, P.C., and Zou, Y. (2008). Wnt signaling in neural circuit assembly. Annu. Rev. Neurosci. *31*, 339–358.

Scharkowski, F., Frotscher, M., Lutz, D., Korte, M., and Michaelsen-Preusse, K. (2018). Altered connectivity and synapse maturation of the hippocampal mossy fiber pathway in a mouse model of the fragile X syndrome. Cereb. Cortex *28*, 852–867.

Schmid, A., Hallermann, S., Kittel, R.J., Khorramshahi, O., Frölich, A.M.J., Quentin, C., Rasse, T.M., Mertel, S., Heckmann, M., and Sigrist, S.J. (2008). Activity-dependent site-specific changes of glutamate receptor composition *in vivo*. Nat. Neurosci. *11*, 659–666.

Schmid, A., Qin, G., Wichmann, C., Kittel, R.J., Mertel, S., Fouquet, W., Schmidt, M., Heckmann, M., and Sigrist, S.J. (2006). Non-NMDA-type glutamate receptors are essential for maturation but not for initial assembly of synapses at *Drosophila* neuromuscular junctions. J. Neurosci. *26*, 11267–11277.

Sheffler-Collins, S.I., and Dalva, M.B. (2012). EphBs: an integral link between synaptic function and synaptopathies. Trends Neurosci. *35*, 293–304.

Shellenbarger, D.L., and Mohler, J.D. (1975). Temperature-sensitive mutations of the notch locus in Drosophila melanogaster. Genetics *81*, 143–162.

Sherrington, R., Rogaev, E.I., Liang, Y., Rogaeva, E.A., Levesque, G., Ikeda, M., Chi, H., Lin, C., Li, G., Holman, K., et al. (1995). Cloning of a gene bearing missense mutations in early-onset familial Alzheimer's disease. Nature *375*, 754–760.

Söderberg, O., Gullberg, M., Jarvius, M., Ridderstråle, K., Leuchowius, K.J., Jarvius, J., Wester, K., Hydbring, P., Bahram, F., Larsson, L.G., et al. (2006). Direct observation of individual endogenous protein complexes *in situ* by proximity ligation. Nat. Methods *3*, 995–1000.

Speese, S.D., Ashley, J., Jokhi, V., Nunnari, J., Barria, R., Li, Y., Ataman, B., Koon, A., Chang, Y.T., Li, Q., et al. (2012). Nuclear envelope budding enables large ribonucleoprotein particle export during synaptic Wnt signaling. Cell *149*, 832–846.

Stempfle, D., Kanwar, R., Loewer, A., Fortini, M.E., and Merdes, G. (2010). *In vivo* reconstitution of γ-secretase in drosophila results in substrate specificity. Mol. Cell. Biol. *30*, 3165–3175.

Suzuki, K., Hayashi, Y., Nakahara, S., Kumazaki, H., Prox, J., Horiuchi, K., Zeng, M., Tanimura, S., Nishiyama, Y., Osawa, S., et al. (2012). Activity-dependent proteolytic cleavage of Neuroligin-1. Neuron *76*, 410–422.

Sweeney, L.B., Couto, A., Chou, Y.H., Berdnik, D., Dickson, B.J., Luo, L., and Komiyama, T. (2007). Temporal target restriction of olfactory receptor neurons by Semaphorin-1a/PlexinA-mediated axon-axon interactions. Neuron *53*, 185–200.

Tabuchi, K., Chen, G., Südhof, T.C., and Shen, J. (2009). Conditional forebrain inactivation of nicastrin causes progressive memory impairment and age-related neurodegeneration. J. Neurosci. *29*, 7290–7301.

Taoufik, E., Kouroupi, G., Zygogianni, O., and Matsas, R. (2018). Synaptic dysfunction in neurodegenerative and neurodevelopmental diseases: an overview of induced pluripotent stem-cell-based disease models. Open Biol. *8*, 180138.

Tapia-Rojas, C., and Inestrosa, N.C. (2018). Loss of canonical Wnt signaling is involved in the pathogenesis of Alzheimer's disease. Neural Regen. Res. *13*, 1705–1710.

Tea, J.S., Chihara, T., and Luo, L. (2010). Histone deacetylase Rpd3 regulates olfactory projection neuron dendrite targeting via the transcription factor Prospero. J. Neurosci. *30*, 9939–9946.

Thurmond, J., Goodman, J.L., Strelets, V.B., Attrill, H., Gramates, L.S., Marygold, S.J., Matthews, B.B., Millburn, G., Antonazzo, G., Trovisco, V., et al. (2019). FlyBase 2.0: the next generation. Nucleic Acids Res. *47*, D759–D765.

Toth, A.B., Terauchi, A., Zhang, L.Y., Johnson-Venkatesh, E.M., Larsen, D.J., Sutton, M.A., and Umemori, H. (2013). Synapse maturation by activity-dependent ectodomain shedding of SIRPα. Nat. Neurosci. *16*, 1417–1425.

Vasin, A., Sabeva, N., Torres, C., Phan, S., Bushong, E.A., Ellisman, M.H., and Bykhovskaia, M. (2019). Two pathways for the activity-dependent growth and differentiation of synaptic boutons in drosophila. eNeuro *6*, 0060–19.2019.

Venken, K.J.T., Schulze, K.L., Haelterman, N.A., Pan, H., He, Y., Evans-Holm, M., Carlson, J.W., Levis, R.W., Spradling, A.C., Hoskins, R.A., et al. (2011b). MiMIC: a highly versatile transposon insertion resource for engineering *Drosophila melanogaster* genes. Nat. Methods *8*, 737–743.

Venken, K.J.T., Simpson, J.H., and Bellen, H.J. (2011a). Genetic manipulation of genes and cells in the nervous system of the fruit fly. Neuron *72*, 202–230.

Vonhoff, F., and Keshishian, H. (2017). Activity-dependent synaptic refinement: new insights from *Drosophila*. Front. Syst. Neurosci. *11*, 23.

Vosshall, L.B., Wong, A.M., and Axel, R. (2000). An olfactory sensory map in the fly brain. Cell *102*, 147–159.

Wang, S., Yoo, S.H., Kim, H.Y., Wang, M., Zheng, C., Parkhouse, W., Krieger, C., and Harden, N. (2015). Detection of *in situ* protein-protein complexes at the drosophila larval neuromuscular junction using proximity ligation assay. J. Vis. Exp. *95*, 52139.

Wegener, S., Buschler, A., Stempel, A.V., Kang, S.J., Lim, C.S., Kaang, B.K., Shoichet, S.A., Manahan-Vaughan, D., and Schmitz, D. (2018). Defective synapse maturation and enhanced synaptic plasticity in shank2 Δex7–/– mice. eNeuro *5*, 1–10.

Wolfe, M.S. (2009). γ-secretase in biology and medicine. Semin. Cell Dev. Biol. *20*, 219–224.

Xie, T., Yan, C., Zhou, R., Zhao, Y., Sun, L., Yang, G., Lu, P., Ma, D., and Shi, Y. (2014). Crystal structure of the γ-secretase component nicastrin. Proc. Natl. Acad. Sci. USA *111*, 13349–13354.

Yang, S., Wu, Y., Xu, T.-H., de Waal, P.W., He, Y., Pu, M., Chen, Y., DeBruine, Z.J., Zhang, B., Zaidi, S.A., et al. (2018). Crystal structure of the Frizzled 4 receptor in a ligand-free state. Nature *560*, 666–670.

Ye, Y., Lukinova, N., and Fortini, M.E. (1999). Neurogenic phenotypes and altered notch processing in drosophila presenilin mutants. Nature *398*, 525–529.

Zhang, C., Wu, B., Beglopoulos, V., Wines-Samuelson, M., Zhang, D., Dragatsis, I., Südhof, T.C., and Shen, J. (2009). Presenilins are essential for regulating neurotransmitter release. Nature *460*, 632–636.

Zinsmaier, K.E., Eberle, K.K., Buchner, E., Walter, N., and Benzer, S. (1994). Paralysis and early death in cysteine string protein mutants of *Drosophila*. Science *263*, 977–980.

Zito, K., Parnas, D., Fetter, R.D., Isacoff, E.Y., and Goodman, C.S. (1999). Watching a synapse grow: noninvasive confocal imaging of synaptic growth in *Drosophila*. Neuron *22*, 719–729.

Zoghbi, H.Y., and Bear, M.F. (2012). Synaptic dysfunction in neurodevelopmental disorders associated with autism and intellectual disabilities. Cold Spring Harb. Perspect. Biol. *4*, a009886.

Zoltowska, K.M., Maesako, M., Lushnikova, I., Takeda, S., Keller, L.J., Skibo, G., Hyman, B.T., and Berezovska, O. (2017). Dynamic presenilin 1 and synaptotagmin 1 interaction modulates exocytosis and amyloid β production. Mol. Neurodegener. *12*, 15.

Zou, Y. (2020). Breaking symmetry - cell polarity signaling pathways in growth cone guidance and synapse formation. Curr. Opin. Neurobiol. *63*, 77–86.

Please cite this article in press as: Restrepo et al., γ-secretase promotes *Drosophila* postsynaptic development through the cleavage of a Wnt receptor, Developmental Cell (2022), https://doi.org/10.1016/j.devcel.2022.05.006

STAR★METHODS

KEY RESOURCES TABLE

REAGENT or RESOURCE	SOURCE	IDENTIFIER
Antibodies		
mouse anti-Dlg	Developmental Studies Hybridoma Bank	Cat# 4F3 anti-discs large; RRID: AB_528203
rabbit anti-Presenilin	Goate Lab; (Nowotny et al., 2000)	N/A
rabbit anti-Nicastrin	This study	N/A
rabbit anti-Dlg	Budnik Lab; (Koh et al., 1999)	RRID: AB_2568354
mouse anti-myc	Developmental Studies Hybridoma Bank	Cat# 9E 10; RRID: AB_2266850
rabbit anti-myc	Thermo Fisher Scientific	Cat# PA5-85185; RRID: AB_2792331
mouse anti-α-spectrin	Developmental Studies Hybridoma Bank	Cat# 3A9 (323 or M10-2); RRID: AB_528473
mouse anti-Brp	Developmental Studies Hybridoma Bank	Cat# nc82; RRID: AB_2314866
rabbit anti-GluRIIC	DiAntonio Lab; (Marrus et al., 2004)	RRID: AB_2568754
rabbit anti-Syt I	Reist Lab; (Mackler et al., 2002)	N/A
mouse anti-CSP	Developmental Studies Hybridoma Bank	Cat# DCSP-2 (6D6); RRID: AB_528183
rabbit anti-dsRed	TaKaRa Bio	Cat# 632496; RRID: AB_10013483
chicken anti-GFP	Aves Labs	Cat# GFP-1020; RRID: AB_10000240
rat anti-N-Cadherin	Developmental Studies Hybridoma Bank	Cat# DN-Ex #8; RRID: AB_528121
rabbit anti Fz2-N	Budnik Lab; (Reichsman et al., 1996)	N/A
rabbit anti Fz2-C	Budnik Lab; (Reichsman et al., 1996)	N/A
mouse anti Lamin C	Developmental Studies Hybridoma Bank	Cat# lc28.26; RRID: AB_528339
mouse anti-FLAG M2	Sigma-Aldrich	Cat# F1804; RRID: AB_262044
rabbit anti-FLAG	Sigma-Aldrich	Cat# F7425; RRID: AB_439687
rabbit anti-Wingless	Budnik Lab; (Packard et al., 2002)	N/A
rabbit anti-Rab5	abCam	Cat# ab31261; RRID: AB_882240
mouse anti-Rab7	Developmental Studies Hybridoma Bank	Cat# Rab7; RRID: AB_2722471
rabbit anti-Importin-β11	Schwarz Lab (Higashi-Kovtun et al., 2010)	N/A
Alexa Fluor 488-AffiniPure Donkey Anti-Mouse IgG	Jackson ImmunoResearch Labs	Cat# 715-545-151; RRID: AB_2341099
Donkey Anti-Chicken IgY Antibody (FITC)	Jackson ImmunoResearch Labs	Cat# 703-095-155; RRID: AB_2340356
Alexa Fluor 488-AffiniPure Donkey Anti-Rat IgG	Jackson ImmunoResearch Labs	Cat# 712-545-153; RRID: AB_2340684
Alexa Fluor 488-AffiniPure Donkey Anti-Rabbit IgG	Jackson ImmunoResearch Labs	Cat# 711-545-152; RRID: AB_2313584
Alexa Fluor 647 AffiniPure Donkey Anti-Mouse IgG	Jackson ImmunoResearch Labs	Cat# 715-605-151; RRID: AB_2340863
Alexa Fluor 647 AffiniPure Donkey Anti-Chicken IgG	Jackson ImmunoResearch Labs	Cat# 103-605-155; RRID: AB_2337392
Alexa Fluor 647 AffiniPure Donkey Anti-Rat IgG	Jackson ImmunoResearch Labs	Cat# 712-605-153; RRID: AB_2340694
Alexa Fluor 647 AffiniPure Donkey Anti-Rabbit IgG	Jackson ImmunoResearch Labs	Cat# 711-605-152; RRID: AB_2492288
Alexa Fluor 568 Goat Anti-Mouse IgG	Thermo Fisher Scientific	Cat# A-11004; RRID: AB_2534072
Alexa Fluor 568 Goat Anti-Rabbit IgG	Thermo Fisher Scientific	Cat# A-11011; RRID: AB_143157
Alexa Fluor 568 Goat Anti-Rat IgG	Thermo Fisher Scientific	Cat# A-11077; RRID: AB_2534121
Alexa Fluor 568 Goat Anti-Chicken IgG	Thermo Fisher Scientific	Cat# A-11041; RRID: AB_2534098
FITC AffiniPure Goat Anti-Horseradish Peroxidase	Jackson ImmunoResearch Labs	Cat# 123-095-021; RRID: AB_2314647

(*Continued on next page*)

Please cite this article in press as: Restrepo et al., γ-secretase promotes *Drosophila* postsynaptic development through the cleavage of a Wnt receptor, Developmental Cell (2022), https://doi.org/10.1016/j.devcel.2022.05.006

Continued

REAGENT or RESOURCE	SOURCE	IDENTIFIER
Cy3 AffiniPure Goat Anti-Horseradish Peroxidase	Jackson ImmunoResearch Labs	Cat# 123-165-021; RRID: AB_2338959
Alexa Fluor 647 AffiniPure Goat Anti-Horseradish Peroxidase	Jackson ImmunoResearch Labs	Cat# 123-605-021; RRID: AB_2338967
Alexa Fluor 546 Phalloidin	Sigma Aldrich	Cat# A-22283; RRID: AB_2632953
mouse anti-α-tubulin DM1a	Sigma-Aldrich	Cat# T9026; RRID: AB_477593
Peroxidase AffiniPure Donkey Anti-Mouse IgG	Jackson ImmunoResearch Labs	Cat# 715-035-151; RRID: AB_2340771
Experimental models: Organisms / strains		
psn^{143}	Bloomington Drosophila Stock Center; (Mahoney et al., 2006)	Cat# 8297; RRID: BDSC_8297
psn^{C4}	Bloomington Drosophila Stock Center; (Lukinova et al., 1999; Ye et al., 1999)	Cat# 63238; RRID: BDSC_63238
psn^{l2}	Bloomington Drosophila Stock Center; (Lukinova et al., 1999; Ye et al., 1999)	Cat# 5463; RRID: BDSC_5463
nct^{A7}	Bloomington Drosophila Stock Center; (Hu et al., 2002)	Cat# 41781; RRID: BDSC_41781
nct^{E3}	Bloomington Drosophila Stock Center; (Hu et al., 2002)	Cat# 63241; RRID: BDSC_63241
nct^{l2}	Fortini Lab; (Hu et al., 2002)	N/A
aph-1^{D35}	Bloomington Drosophila Stock Center; (Hu and Fortini, 2003)	Cat# 63242; RRID: BDSC_63242
Df(2L)Exel6277	Bloomington Drosophila Stock Center; (Artavanis-Tsakonas, 2004)	Cat# 7744; RRID: BDSC_7744
pen-2^{MI02639}	Bloomington Drosophila Stock Center; (Venken et al., 2011b)	Cat# 36019; RRID: BDSC_36019
dfz2^{C1}	Mosca Lab; (Chen and Struhl, 1999)	N/A
Df(3L)ED4782	Bloomington Drosophila Stock Center; (Mathew et al., 2005)	Cat# 8082; RRID: BDSC_8082
appl^{D}	Bloomington Drosophila Stock Center; (Luo et al., 1992)	Cat# 43632; RRID: BDSC_43632
N^{ts1}	Bloomington Drosophila Stock Center; (Shellenbarger and Mohler, 1975)	Cat# 2533; RRID: BDSC_2533
imp-β11^{70}	Mosca Lab; (Higashi-Kovtun et al., 2010)	N/A
msk^{5}	Bloomington Drosophila Stock Center; (Lorenzen et al., 2001)	Cat# 23879; RRID: BDSC_23879
Df(2R)Δm22	Mosca Lab; (Boll and Noll, 2002; Higashi-Kovtun et al., 2010)	N/A
Df(X)ten-a	Mosca Lab; (Mosca et al., 2012)	N/A
UAS-Fz2-FLAG	Mosca Lab; (Piddini et al., 2005)	N/A
UAS-Psn-Nmyc	Bloomington Drosophila Stock Center; (Stempfle et al., 2010)	Cat# 63209; RRID: BDSC_63209
UAS-Nct-2myc	Bloomington Drosophila Stock Center; (Stempfle et al., 2010)	Cat# 63215; RRID: BDSC_63215
UAS-Aph1-V5	Bloomington Drosophila Stock Center; (Stempfle et al., 2010)	Cat# 63216; RRID: BDSC_63216
UAS-Pen2-flag	Bloomington Drosophila Stock Center; (Stempfle et al., 2010)	Cat# 64067; RRID: BDSC_64067
UAS-Fz2-FL	Budnik Lab; (Mathew et al., 2005)	N/A
UAS-Fz2-ΔKTLES	Budnik Lab; (Mathew et al., 2005)	N/A
UAS-myc-NLS-Fz2-C	Budnik Lab; (Mathew et al., 2005)	N/A
UAS-NLS-GFP	Bloomington Drosophila Stock Center; (Allan et al., 2003)	Cat# 4775; RRID: BDSC_4775

(*Continued on next page*)

Please cite this article in press as: Restrepo et al., γ-secretase promotes *Drosophila* postsynaptic development through the cleavage of a Wnt receptor, Developmental Cell (2022), https://doi.org/10.1016/j.devcel.2022.05.006

Continued

REAGENT or RESOURCE	SOURCE	IDENTIFIER
UAS-DshDIX	Axelrod Lab; (Axelrod et al., 1998)	N/A
UAS-Arm^{S10}	Yashi Ahmed; (Pai et al., 1997)	N/A
UAS-kuz-DN	Mosca Lab; (Pan and Rubin, 1997)	Cat# 6578; RRID: BDSC_6578
UAS-psn-IR-43082	Vienna Drosophila Resource Center; (Dietzl et al., 2007)	FlyBase Cat# FBst0464909; RRID: FlyBase_FBst0464909
UAS-aph-1-IR-16820	Vienna Drosophila Resource Center; (Dietzl et al., 2007)	FlyBase Cat# FBst0452426; RRID: FlyBase_FBst0452426
UAS-mam-IR-102091	Vienna Drosophila Resource Center; (Dietzl et al., 2007)	FlyBase Cat# FBst0468065; RRID: FlyBase_FBst0468065
UAS-nct-IR-JF02648	Bloomington Drosophila Stock Center; (Hu et al., 2017)	Cat# 27498; RRID: BDSC_27498
UAS-pen-2-IR-JF02608	Bloomington Drosophila Stock Center; (Hu et al., 2017)	Cat# 27298; RRID:BDSC_27298
elav^{C155}-GAL4	Bloomington Drosophila Stock Center; (Lin and Goodman, 1994)	Cat# 458; RRID: BDSC_458
elav-GAL4	Bloomington Drosophila Stock Center; (Luo et al., 1994)	Cat# 8760; RRID: BDSC_8760
DMef2-GAL4	Bloomington Drosophila Stock Center; (Lilly et al., 1995)	Cat# 27390; RRID: BDSC_27390
Or67d-GAL4	Mosca Lab; (Kurtovic et al., 2007)	N/A
Or47b-GAL4	Bloomington Drosophila Stock Center; (Vosshall et al., 2000)	Cat# 9984; RRID: BDSC_9984
pebbled-GAL4	Mosca Lab; (Sweeney et al., 2007)	N/A
psn^{H185R}	This study	N/A
psn^{G228D}	This study	N/A
UAS-HA-Fz2-FLAG	This study	N/A
UAS-Fz2+AAAAA	This study	N/A
Chemicals		
L-685,458	Tocris Bioscience	Cat# 2627
Papain	Worthington Biochemical Corporation	Cat# LS003124
Hanks Balanced Salt Solution	Sigma-Aldrich	Cat# 55037C-1000ML
Trypsin Inhibitor	Sigma-Aldrich	Cat# 10109886001
Neurobasal™ Medium	Thermo Fisher Scientific	Cat# 21103049
B-27™ Plus Supplement	Thermo Fisher Scientific	Cat# A3582801
L-Glutamine	Thermo Fisher Scientific	Cat# 21051024
Penicillin-Streptomycin	Thermo Fisher Scientific	Cat# 15140122
Lipofectamine™ 2000 Transfection Reagent	Thermo Fisher Scientific	Cat# 11668019
Commercial assays/kits		
SuperSignal™ West Femto Maximum Sensitivity Substrate	Thermo Fisher Scientific	Cat# 34095
DuoLink Mouse Rabbit in situ PLA Kit	Sigma-Aldrich	Cat# DUO92101
Cell lines		
Primary rat cortical neurons	Charles River	N/A
Recombinant DNA/plasmids		
pBS-LD10629	Drosophila Genomic Resource Center	Cat# 5162
pUAST-W-tFHAH-attB	Mosca Lab; (Mosca et al., 2012)	N/A
pBS-FZ2.FLAG	This study	N/A
pENTR-D-TOPO	Thermo Fisher Scientific	Cat# K242020
pENTR-FLAG#5.ORF	This study	N/A
pENTR-HA-FZ2-FLAG	This study	N/A

(*Continued on next page*)

Please cite this article in press as: Restrepo et al., γ-secretase promotes *Drosophila* postsynaptic development through the cleavage of a Wnt receptor, Developmental Cell (2022), https://doi.org/10.1016/j.devcel.2022.05.006

Continued

REAGENT or RESOURCE	SOURCE	IDENTIFIER
pUAST-Gateway-attB	Mosca Lab; (Tea et al., 2010)	N/A
pUAST-Fz2+AAAAA-attB	This study	N/A
pUAST-HA-FZ2-FLAG	This study	N/A
Software		
ZEN 2.3 software	Carl Zeiss	ZEN Digital Imaging for Light Microscopy, RRID:SCR_013672
Adobe Photoshop	Adobe Systems	Adobe Photoshop, RRID:SCR_014199
Adobe Illustrator	Adobe Systems	Adobe Illustrator, RRID:SCR_010279
ImageJ	NIH	ImageJ, RRID:SCR_003070
Imaris	Oxford Instruments	Imaris, RRID:SCR_007370
Prism	GraphPad Software, Inc	GraphPad Prism, RRID:SCR_002798
SnapGene	SnapGene	SnapGene, RRID:SCR_015052

RESOURCE AVAILABILITY

Lead contact

Requests for any resources or reagents should be addressed to the lead contact, Timothy J. Mosca (timothy.mosca@jefferson.edu).

Materials availability

All plasmids, transgenic flies, antibodies, and custom reagents created for this study are available upon request to the lead contact.

Data and code availability

- Original data including image files, Western blots, or data tables are available from the lead contact on reasonable request.
- No new code was created for this study.
- Any additional information required to repeat the experiments or reanalyze the data is available from the lead contact on reasonable request.

EXPERIMENTAL MODEL AND SUBJECT DETAILS

Drosophila stocks and transgenic strains

All control genotypes, mutant combinations, transgenic lines, manipulations, and crosses were maintained on cornmeal medium (Archon Scientific, Durham, NC) at 25°C and 60% relative humidity with a 12/12 light/dark cycle in specialized incubators (Darwin Chambers, St. Louis, MO). N^{TS} mutants were raised as described (De Bivort et al., 2009). All genetic components (mutant alleles, transgenes, drivers, etc.) were maintained over larvally selectable balancer chromosomes to enable facile identification at the appropriate life stage. The following mutant alleles were used: psn^{143} (Mahoney et al., 2006), psn^{C4}, psn^{I2} (Lukinova et al., 1999; Ye et al., 1999), nct^{A7}, nct^{E3}, nct^{J2} (Hu et al., 2002), $aph\text{-}1^{D35}$ (Hu and Fortini, 2003), *Df(2L)Exel6277* (as $aph\text{-}1^{Df}$) (Artavanis-Tsakonas, 2004), $pen\text{-}2^{MI02639}$ (Venken et al., 2011b), $dfz2^{C1}$ (Chen and Struhl, 1999), Df(3L)ED4782 (as $dfz2^{Df}$) (Mathew et al., 2005), $appl^{D}$ (Luo et al., 1992), N^{ts1} (De Bivort et al., 2009; Shellenbarger and Mohler, 1975), msk^{5} (Lorenzen et al., 2001), $imp\text{-}\beta11^{70}$ (Higashi-Kovtun et al., 2010), Df(2R)Δm22 (as $imp\text{-}\beta11^{Df}$) (Boll and Noll, 2002; Higashi-Kovtun et al., 2010), *Df(X)ten-a* (Mosca et al., 2012). The following UAS transgenes were used: *UAS-Fz2-FLAG* (Piddini et al., 2005), *UAS-Psn-Nmyc*, *UAS-Nct-2myc*, *UAS-Aph1-V5*, *UAS-Pen2-2flag* (Stempfle et al., 2010), *UAS-Fz2-FL*, *UAS-Fz2-ΔKTLES*, *UAS-myc-NLS-Fz2-C* (Mathew et al., 2005), UAS-Arm^{S10} (Pai et al., 1997), *UAS-NLS-GFP* (Allan et al., 2003), *UAS-Dsh-DIX* (Axelrod et al., 1998), *UAS-kuz-DN* (Pan and Rubin, 1997), *UAS-psn-IR-43082*, *UAS-aph-1-IR-16820*, *UAS-mam-IR-102091* (Dietzl et al., 2007), *UAS-nct-IR-JF02648*, *UAS-pen-2-IR-JF02608* (Hu et al., 2017). The following GAL4 driver lines were used to achieve tissue-specific expression: $elav^{C155}$*-GAL4* (Lin and Goodman, 1994) or *elav-GAL4* (Luo et al., 1994) (pan-neuronal expression), *DMef2-GAL4* (Lilly et al., 1995) (pan-muscle expression) *Or67d-GAL4* (Kurtovic et al., 2007) (DA1 ORN expression), *Or47b-GAL4* (Vosshall et al., 2000) (VA1lv ORN expression), *pebbled-GAL4* (Sweeney et al., 2007) (pan-ORN expression). Specific genotypes are denoted in Table S2.

Construction of psn^{H185R} and psn^{G228D}

The sequences of human Presenilin1 (PSEN1) and *Drosophila* Presenilin (Psn) were aligned using SnapGene software (Insightful Science, San Diego, CA) and the equivalent residues from known patient mutations (Lanoiselée et al., 2017) identified. Psn H185R was selected as the *Drosophila* equivalent to H163R and G228D as the *Drosophila* equivalent to human PSEN1 G206D. We used CRISPR/Cas9 editing (Gratz et al., 2015) with WellGenetics, Inc. (Taipei City, Taiwan) to make a custom-designed gRNA and accompanying

construct to introduce the specific mutation. Four lines were obtained for each allele and sequenced to confirm the presence of the change. One line bearing the mutation was stabilized over a third chromosome balancer and used for further experiments.

Cloning of Fz2 constructs and transgenic line production

The HA- and FLAG-tagged Fz2 construct has a 3X HA tag inserted at amino acid position 220 (between the cysteine rich domain and the transmembrane domain) and a C-terminal 3X-FLAG tag. Previous work suggested those locations did not interfere with normal protein function (Boutros et al., 2000; Piddini et al., 2005). These were inserted into sequence amplified from a full length BDGP-Gold Fz2 cDNA clone (LD10629 in pBluescript) from the *Drosophila* Genomics Resource Center (DGRC, supported by NIH grant 2P40OD010949). All PCR amplification steps used the high fidelity Q5 Polymerase (New England Biolabs) and primers from Integrated DNA Technology (Coralville, IA). The FLAG tag was amplified from pUAST-W-tFHAH-attB (Mosca et al., 2012) and cloned into LD10629 which was linearized and assembled using In-Fusion HD (Takara Bio). This resulted in plasmid pBS-FZ2.FLAG which was used to amplify the dFZ2 ORF with the FLAG tag for cloning into the Gateway entry vector pENTR-D-TOPO (Thermo Fisher Scientific). This step eliminated most of the dFZ2 5' and 3' UTRs while maintaining the presumptive Kozak sequence adjacent to the start codon. Following In-Fusion assembly, the resulting plasmid, pENTR-FLAG#5.ORF, was used to engineer the HA tag between the dFZ2 cysteine rich and transmembrane domains. The HA epitope tag (amplified from pUAST-W-tFHAH-attB) was inserted by In-Fusion cloning of multiple fragments in pENTR-FLAG#5.ORF. Positive clones were screened and verified by PCR diagnostics and Sanger sequencing. This gave pENTR-HA-FZ2-FLAG which was then used in a Gateway LR reaction with the pUAST-Gateway-attB vector (Tea et al., 2010) to generate pUAST-HA-FZ2-FLAG. This plasmid was used to generate transgenic flies (BestGene, Chino Hills, CA) with the construct integrated into the VK00037 docking site. To make the Fz2-5AAAAA, we first modeled the structure of *Drosophila* Fz2 using a transmembrane protein topology prediction with hidden Markov model to predict transmembrane regions (TMHMM; Krogh et al., 2001) and the crystal structure of human Fz4 (PBD: 6BD4; Yang et al., 2018) using SWISS-MODEL and visualized the resultant model prediction using PyMol 2.3.1 (Schrodinger, Inc). We then inserted 5 alanines between residues 607 (the end of the 7th transmembrane domain) and 608 (the beginning of the KTLES sequence) as above using a UAS-DFz2 plasmid (Mathew et al., 2005) as template. The DFz2 ORF was then amplified and cloned into the pUAST-Gateway-attB vector using a Gateway LR reaction to generate pUAST-Fz2+AAAAA-attB. Transgenic flies were generated (BestGene, Chino Hills, CA) with the construct integrated into the attP40 docking site.

METHOD DETAILS

RNAi protease screen

Fz2 cleavage occurs at a consensus (KTLES) glutamyl-endopeptidase site (Mathew et al., 2005). We used two GO_MOLECULAR_FUNCTION terms in FlyBase (Thurmond et al., 2019): "endopeptidase" and "metalloprotease" and identified 121 total genes with those predicted molecular functions. From that list, 116 genes had 1 or more RNAi lines available at the Vienna Drosophila Resource Center (VDRC) or the Harvard TRiP Collection (Dietzl et al., 2007; Hu et al., 2017). We omitted the Neprilysin family (26 genes) as its active site faces the extracellular space (Nalivaeva and Turner, 2013) and DFz2-C cleavage is expected to occur in the cytoplasm. We obtained RNAi lines for the remaining 93 candidates as well as 3 controls: two positive controls - dfz2 (Mathew et al., 2005) and *trol* (Kamimura et al., 2013) - known to impair postsynaptic development and maturation, and one negative control - GFP. Because Fz2 cleavage occurs in the muscle, we conducted the screen by driving each RNAi line specifically in muscles using the DMef2-GAL4 driver (Lilly et al., 1995). We reasoned that impairing Fz2 cleavage (by blocking the relevant protease) would impair postsynaptic development and maturation similarly to the removal of the Fz2 receptor itself and show similar phenotypes. We screened F1 progeny of crosses between each RNAi line and the DMef2-GAL4 driver (with the experimenter blind to genotype) and quantified "ghost boutons," a hallmark of impaired postsynaptic maturation (Ataman et al., 2006, 2008; Fuentes-Medel et al., 2009; Korkut et al., 2009; Mosca and Schwarz, 2010a; Mosca et al., 2012; Speese et al., 2012). Positive hits were lines that caused a significant increase in ghost boutons over the negative control. For all genotypes, we performed immunocytochemistry in third instar larvae (see below) and stained with antibodies against postsynaptic Dlg and presynaptic HRP. For all genotypes, at least 6 NMJs in 6 larvae were scored. To ensure that any potential defects were not due to destabilization of the synapse, we also scored "footprints," which are retracted synapses that are positive for Dlg staining and negative for HRP staining (Eaton and Davis, 2005; Pielage et al., 2005, 2008). Only four genes showed a significant increase in ghost boutons over the negative control: *dfz2* and *trol* (the positive controls), *psn*, and *nct*.

Cleavage assay, Western blot, and SDS-PAGE analyses

UAS-Fz2-FLAG was expressed in muscles using *DMef2-GAL4* in a wild-type, *imp-β11* mutant, *psn* mutant, or *nct* mutant background. Lysates were prepared from partially dissected third instar larval body walls as described (Mosca and Schwarz, 2010a). Proteins were separated on 4-15% Mini-PROTEAN TGX gels (BioRad, Hercules, CA) and transferred to nitrocellulose. Blots were incubated overnight in primary antibodies at 4°C and secondary antibodies at room temperature (21-22°C) for 1 hour. The following primary antibodies were used: mouse anti-FLAG M2 (Sigma-Aldrich, cat. no. F1804, 1:5000) and mouse anti-α-tubulin DM1a (Sigma-Aldrich, cat. no. T9026, 1:10000). HRP-conjugated secondary antibodies were used at 1:10000 (Jackson ImmunoResearch, West Grove, PA). Blots were developed using the SuperSignal West Femto Maximum Sensitivity Substrate Kit (ThermoFisher Scientific, Waltham, MA).

Please cite this article in press as: Restrepo et al., γ-secretase promotes *Drosophila* postsynaptic development through the cleavage of a Wnt receptor, Developmental Cell (2022), https://doi.org/10.1016/j.devcel.2022.05.006

Production of Nicastrin antibodies

Custom antibodies were made against a TSKDFTQLTEVNDFKSLNPDSLQ-C peptide corresponding to amino acids 462-484 of the Nicastrin protein (Pacific Immunology Corp., Ramona, CA). Rabbit antisera were affinity-purified against the original immunizing peptide and used at a dilution of 1:500 on wandering third instar larvae (see below). Specificity of the antisera was validated by the absence of signal in $nct^{A7/J2}$ mutant larvae.

Immunocytochemistry

Wandering third instar larvae were dissected and stained as described (Mosca and Schwarz, 2010a). The following primary antibodies were used: mouse anti-Dlg (DSHB, cat. no. mAb4F3, 1:500) (Parnas et al., 2001), rabbit anti-Presenilin (custom, 1:200) (Nowotny et al., 2000), rabbit anti-Nicastrin (custom, 1:500) (this study), rabbit anti-Dlg (custom, 1:40000) (Koh et al., 1999), mouse anti-myc (DSHB, cat. no mAb9E10, 1:100), rabbit anti-myc (ThermoFisher Scientific, cat. no PA5-85185, 1:200), mouse anti-α-spectrin (DSHB, cat. no. mAb3A9, 1:50) (Byers et al., 1987), mouse anti-Brp (DSHB, cat. no. mAbnc82, 1:250) (Laissue et al., 1999), rabbit anti-GluRIIC (custom, 1:2500) (Marrus et al., 2004), rabbit anti-Syt I (custom, 1:4000) (Mackler et al., 2002), mouse anti-CSP (DSHB, cat. no. mAb6D6, 1:100) (Zinsmaier et al., 1994), rabbit anti-dsRed (TaKaRa Bio, cat. no. 632496, 1:250) (Mosca and Luo, 2014), chicken anti-GFP (Aves, cat. no. GFP-1020, 1:1000) (Mosca and Luo, 2014), rat anti-N-Cadherin (DSHB, cat. no. mAbDNEX-8, 1:40) (Iwai et al., 1997), rabbit anti Fz2-N (custom, 1:100) (Reichsman et al., 1996), rabbit anti Fz2-C (custom, 1:200) (Reichsman et al., 1996), mouse anti Lamin C (DSHB, cat. no. mAbLC28.26, 1:200) (Riemer et al., 1995), mouse anti-FLAG M2 (Sigma-Aldrich, cat. no. F1804, 1:500), rabbit anti-FLAG (Sigma-Aldrich, cat. no. F7425, 1:250), rabbit anti-Wingless (custom, 1:200) (Packard et al., 2002), rabbit anti-Rab5 (abCam, cat. no. ab31261, 1:200), mouse anti-Rab7 (DSHB, cat. no. Rab7, 1:100), rabbit anti-Importin-β11 (custom, 1:750) (Higashi-Kovtun et al., 2010). Where noted, monoclonal antibodies were obtained from the Developmental Studies Hybridoma Bank, created by the NICHD of the NIH and maintained at The University of Iowa, Department of Biology. Alexa488-, Alexa647- (Jackson ImmunoResearch, West Grove, PA), and Alexa546-conjugated (ThermoFisher, Waltham, MA) secondary antibodies were used at 1:250. FITC-, Cy3-, or Alexa647-conjugated goat anti-HRP primary antibodies were used at 1:100 (Jackson ImmunoResearch, West Grove, PA). Texas-Red-conjugated phalloidin was used at 1:300 (Sigma Aldrich, St. Louis, MO).

Proximity ligation assay

Larvae were processed as described (Wang et al., 2015) using the DuoLink Mouse Rabbit in situ PLA Kit (Sigma-Aldrich, cat. no. DUO92101, St. Louis, MO). Controls were performed with one or the other epitope-tagged transgene absent or with the probes replaced by water during the first PLA step to ensure that signal observed as not background or bleed-through of channels. To quantify each experiment, an ROI was drawn around the synaptic region and the number of PLA puncta in red were quantified by hand. In the PLA experiments, a significant number of puncta were observed in all cases. In all controls, low levels of background puncta were observed (Figures S5G–S5I), demonstrating interaction specificity. In experiments involving PLA with endogenous antibodies, the secondary antibody was omitted in analogous controls to ensure signal specificity. Larvae were then imaged via confocal microscopy as described (see below).

Imaging and image processing

RNAi screen imaging was conducted on a Leica SP8 confocal microscope (Leica Microsystems, Wetzlar, Germany). All other larvae, adult *Drosophila*, and primary cortical neurons were imaged with a Zeiss LSM880 with Fast AiryScan confocal microscope (Carl Zeiss, Oberlochen, Germany) using a 10X 0.4 NA, 40X 1.4 NA PlanApo, or a 63X 1.4 NA PlanApo lens. Images were processed and quantified as described (Mosca and Schwarz, 2010a; Mosca et al., 2017) and figures constructed using ZEN 2.3 software (Carl Zeiss, Oberlochen, Germany), Adobe Photoshop 2020, and Adobe Illustrator 2020 (Adobe Systems, San Jose, CA).

Behavioral larval crawling assays

Crawling assays were conducted, and peristaltic waves and head sweeps determined, as described (Clark et al., 2018; Fushiki et al., 2016; Humberg et al., 2018; Lnenicka et al., 2003). The experimenter was blind to larval genotype during quantification.

Pharmacological inhibition of γ-secretase *in vivo*

Larvae were raised on small-batch *Drosophila* cornmeal dextrose medium (Department of Biology University of Oregon, 1974) prepared with 5 μM L685,458 (Tocris Bioscience, Minneapolis, MN) and processed as above. This drug has been used *in vivo* as a potent and specific γ-secretase activity blocker (Liu et al., 2018).

Primary neuron culture

Dissociated cortical neurons were prepared from embryonic day 17 Long-Evans rat embryos obtained from timed pregnant rats purchased from Charles River Laboratories, Inc. (Wilmington, MA) and used in accordance with the Guidelines for the Care and Use of Laboratory Animals of the National Institutes of Health and gifted from the lab of Matthew Dalva. Cortices were incubated with 10 μg/mL papain (Worthington Biochemical Corporation) in HBSS for 4 min at 37 °C. Following three washes in HBSS with 0.01 g/mL trypsin inhibitor (Sigma), cortices were triturated with a fire-polished glass Pasteur pipette 5–10 times to obtain a homogeneous cell suspension. Neurons were plated on poly-D-lysine (BD Biosciences, Bedford, MA) and laminin (BD Biosciences)-coated glass coverslips (12 mm; Bellco Glass, Vineland, NJ) in 24-well plates (Corning Life Sciences, Lowell, MA). Neurons were

plated at a density of 6 × 10^5 cells/cm^2 and cultured in Neurobasal media (Invitrogen, Carlsbad, CA) supplemented with B-27 (Invitrogen), 1% glutamine (Invitrogen), and 1% penicillin–streptomycin (Invitrogen) and maintained in a humidified incubator with 5% CO_2 at 37°C.

Neuronal transfection and drug treatment

Neurons were transfected using Lipofectamine 2000 (Invitrogen) after 3 days in vitro. Transfection mixture was prepared (per coverslip) as follows: 0.5 μL Lipofectamine 2000 was added to 50 μL neurobasal medium (without supplement) in a polystyrene tube (USA Scientific). DNA was added to 50 μL neurobasal medium (without supplement) in an Eppendorf tube. After 5 min, the DNA mixture was added to Lipofectamine and incubated at room temperature for 15 min. Conditioned media was removed from the neuronal cultures and replaced with 300 μL of warm neurobasal medium (without supplement). Transfection mixture was added to the neuronal culture and incubated for 2 h at 37 °C and subsequently replaced with filter-sterilized warm conditioned media. For drug treatment, compound L685,458 (Tocris Bioscience, Minneapolis, MN) dissolved in DMSO was added at a final concentration of 2.5 μM once after 7 days in vitro. For the control condition, the same volume of DMSO was added.

Primary neuron immunocytochemistry

After 21 days in vitro, neurons were fixed with 4% paraformaldehyde and 2% sucrose for 10 minutes. Neurons were washed three times with PBS. For antibody labeling, neurons were blocked in PBS plus 5% goat serum and 0.1% Triton (PGT) for 1 hour and then incubated with primary antibodies (GFP; Aves lab) diluted in PGT overnight at 4°C After washing, neurons were incubated Alexa 488 secondary antibodies (Jackson ImmunoResearch or Invitrogen) diluted in PGT for 2 hours at room temperature. Finally, neurons were washed three times with PBS and mounted with Mowiol.

QUANTIFICATION AND STATISTICAL ANALYSIS

Quantification of NMJ synaptic parameters in larval Drosophila

Ghost boutons were quantified as HRP-positive and Dlg-negative and samples blinded during imaging and quantification. All other NMJ parameters (bouton number, muscle size, puncta quantification, synaptic protein level) were quantified as previously described (Mosca and Schwarz, 2010b). Fluorescence intensity was measured with ImageJ (NIH, Bethesda, MD). Comparison of fluorescence levels for various parameters was done on samples that were imaged using identical confocal settings, laser powers, and conditions.

Quantification of synaptic parameters in adult Drosophila

Synaptic puncta (Brp-Short-mStraw) and neurite membrane volume (mCD8-GFP) were imaged, processed, and quantified as described (Mosca and Luo, 2014). All images were obtained as above using a 63X 1.4 NA PlanApo lens and quantified / processed using Imaris Software 9.3.1 (Oxford Instruments, Abingdon, UK) on a custom image processing computer (Digital Storm, Fremont, CA).

Quantification of dendritic spines in primary neuronal culture

Dendritic subtype (stubby, mushroom-headed, thin filopodia) were quantified by hand, according to established methods (Rochefort and Konnerth, 2012). Dendritic spine density was quantified by counting the total number of spines on single neuronal processes and dividing by the total length of the neuronal process. For each cover slip, at least 10-15 processes were quantified, and at least 3 cover slips of each genotype were quantified per genotype.

Statistical analysis

Statistical analysis was performed, and graphical representations prepared using Prism 8.4.3 (GraphPad Software, Inc., La Jolla, CA). In all cases, *n* is expressed as the number of larvae and NMJs analyzed or the number of experiments done. Data for sample size and statistical significance can be found in the figure legends and indicated on graphs in the figures themselves. Throughout the study, the data is expressed as mean ± SEM. Significance between two samples was determined using a two-tailed Student's t-test; significance amongst 3 or more samples was determined using one-way ANOVA with a Dunnett post-hoc test to a control sample and a Bonferroni post-hoc test amongst all samples. Multiple comparisons were corrected for in all cases using a Tukey's post-hoc test. Neural parameters at the NMJ were assumed to follow a Gaussian distribution, consistent with previous literature (Lnenicka and Keshishian, 2000). In each figure, unless otherwise noted, statistical significance is denoted in comparison to control genotypes.

Article

Developmental Cell

γ-secretase promotes *Drosophila* postsynaptic development through the cleavage of a Wnt receptor

Graphical abstract

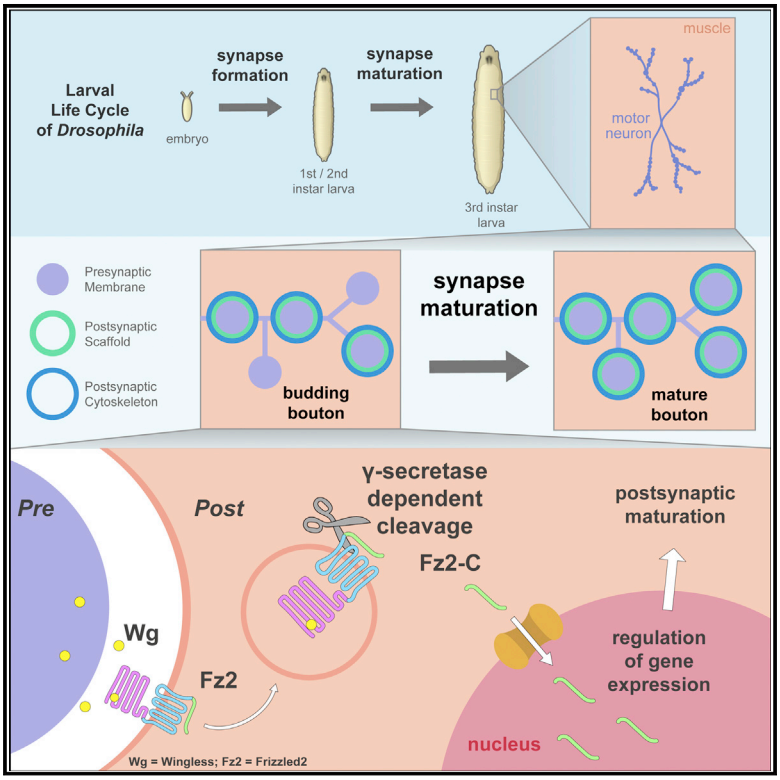

Highlights

- Fz2 receptor cleavage promotes postsynaptic maturation at the *Drosophila* NMJ
- Postsynaptic γ-secretase in development regulates synaptic maturation and function
- γ-secretase influences postsynaptic maturation by enabling the cleavage of Fz2
- AD-linked alleles of *presenilin* in fly show synaptic maturation defects

Authors

Lucas J. Restrepo, Alison T. DePew, Elizabeth R. Moese, ..., Juan Carlos Duhart, Hong Fei, Timothy J. Mosca

Correspondence

timothy.mosca@jefferson.edu

In brief

To form the connections that underlie thought and memory, synapses in the brain must first mature. Restrepo et al. demonstrate that synaptic maturation in *Drosophila* requires the cleavage of the Wnt receptor Fz2 via γ-secretase, a proteolytic complex implicated in Alzheimer's disease. This highlights previously unappreciated connections between neurodevelopmental and neurodegenerative mechanisms.

Restrepo et al., 2022, Developmental Cell *57*, 1–18
July 11, 2022
https://doi.org/10.1016/j.devcel.2022.05.006

CellPress